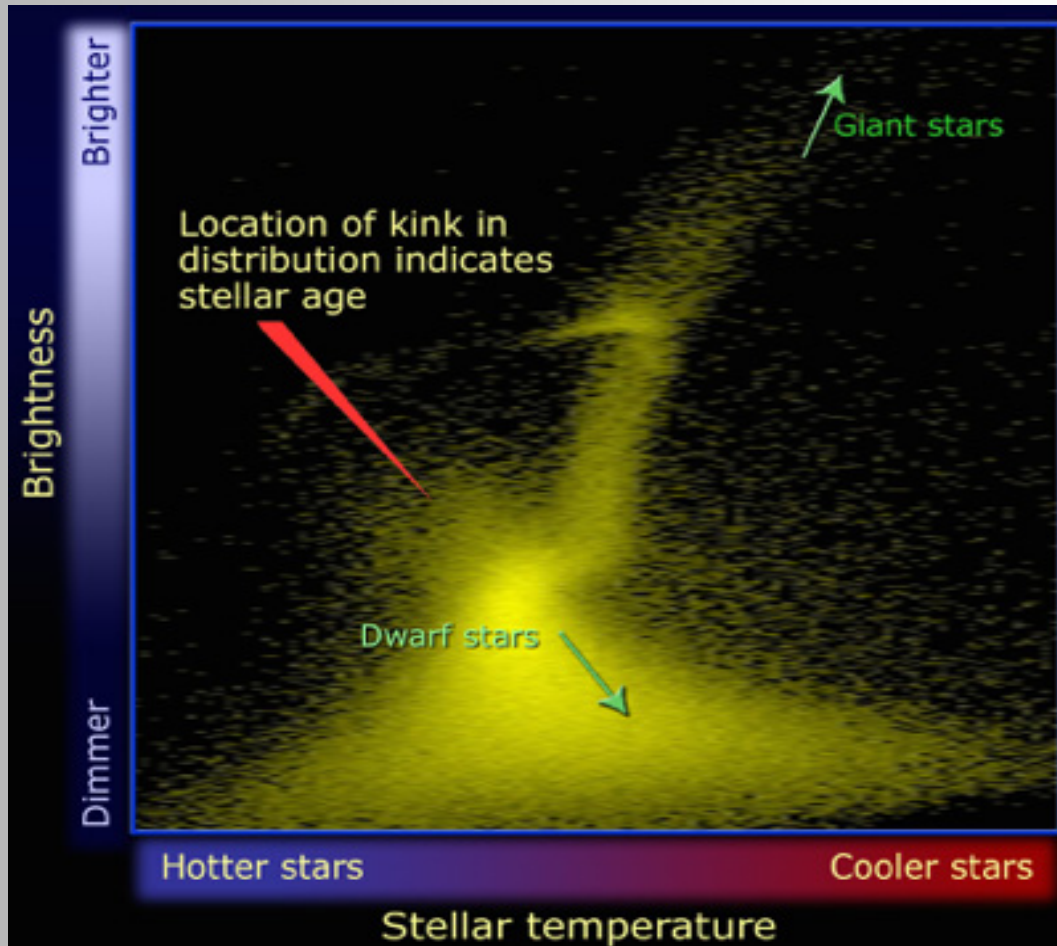


# BAV MAGAZINE SPECTROSCOPY

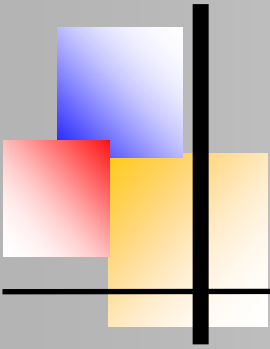


## OF THE GERMAN ORGANIZATION & WORKING GROUP VARIABLE STARS BAV

EDITOR  
BUNDESDEUTSCHE ARBEITSGEMEINSCHAFT  
FÜR VERÄNDERLICHE STERNE E.V. (BAV)  
MUNSTERDAMM 90  
12169 BERLIN

ISSUE No. 11 07/2022 ISSN 2566-5103





# BAV MAGAZINE SPECTROSCOPY



---

## EDITORIAL

From the stars we basically receive only their electromagnetic radiation of different wavelengths, and we “see” essentially only the surface of the radiating bodies. By evaluating the light, we obtain information about:

- the direction of the radiation (positions and movement of the stars)
- the quantity of the radiation (brightness)
- the quality of the radiation (color, spectrum, polarization)

For amateurs, only the narrow band of visible light is easily accessible. In this spectral region, however, both the brightness (photometry) and the spectra of the objects can be examined. Today's amateur astronomy, with its instrumental and computer-assisted equipment, enjoys observation possibilities that were reserved exclusively for professional astronomers until a few years ago.

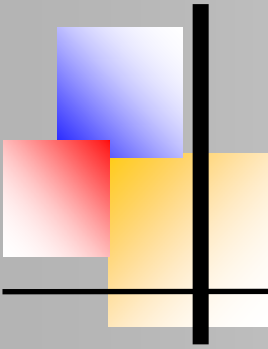
Thanks to the development of CCD technology, the types of observational perspectives have become much more varied. For example, in the area of variable star observation, there are many new possibilities in addition to already existing approaches.

Professional variable star research employs techniques and observation methods to study the physics and atmospheres of the stars in a holistic manner, considering all aspects and occurrences. Thus, this means that the collected radiation must be understood as a complex storage medium of the physical processes on and in the observed star.

This is appropriate for the intensity of the light, as well as for its spectral composition. The linking of brightness measurements and spectroscopy, a matter of course in professional astronomy, reflects this connection.

Along with brightness changes that occur in variable stars (which can occur quite frequently) variable changes in the state of the stars also can take place and often are revealed in the corresponding spectrum.

Ernst Pollmann



# BAV MAGAZINE SPECTROSCOPY



## Imprint

The BAV MAGAZINE SPECTROSCOPY appears half-yearly from June 2017. Responsibility for publication: German Working Group for Variable Stars e.V. (BAV), Munsterdamm 90, 12169 Berlin

## Editorial

Ernst Pollmann, 51375 Leverkusen, Emil-Nolde-Straße 12, ernst-pollmann@t-online.de  
Lienhard Pagel, 18311, Klockenhagen Mecklenburger Str. 87, lienhard.pagel@t-online.de  
Roland Bücke, 21035 Hamburg, Anna von Gierke Ring 147, rb@buecke.de

The authors are responsible for their contributions.

Coverpicture:

[https://cococubed.asu.edu/pix\\_pages/hr\\_diagram.shtml](https://cococubed.asu.edu/pix_pages/hr_diagram.shtml)

## Content

## Page

### E. Pollmann: Editorial

M. Schwarz: SpectroCalc2 – another way to reduce your spectra.....1

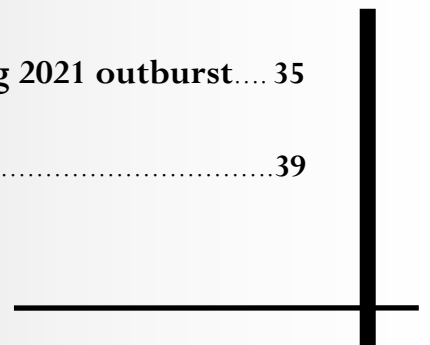
E. Wischnewski: V1405 Cas Nova 2021-  
About the nature of a multi-maxima nova.....6

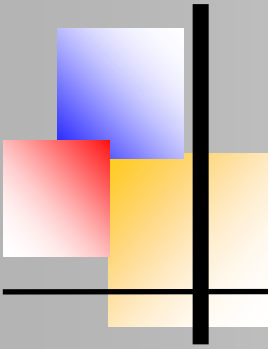
R. K. Buchheim, F. Sims, J. Martin, A. Stiewing, G. Walker:  
Spectroscopy of Stellar Flares.....23

M. König: Spectroscopy of the Seyfert Galaxy NGC 2410..... 31

M. Kolb: RS Oph – Variation of narrow Na D lines during 2021 outburst.... 35

E. Pollmann: The V/R-Ratio in zeta Tau.....39





## SpectroCalc2 – another way to reduce your spectra

Manfred Schwarz, Wiener-Neustadt (Österreich)

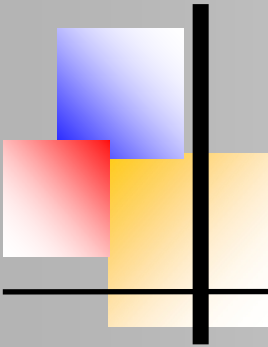


I have been interested in spectroscopy since 2014. In the beginning, like many other amateur spectroscopists, I encountered various data reduction problems. You find on the internet different tools for data reduction: some of them are very professional but complex to use; some of them are not transparent and often they use dubious algorithms. In order to get reasonable results, it was necessary to use different software tools for different steps of data reduction. That was too time consuming for me, so I decided to develop a software tool. After a couple years, the result was the SpectroCalc2 application.

### The Way to the Goal

The data reduction process, from the 2D images taken, to the finished spectrum, is generally well known and will not be described in detail in this article. SpectroCalc2 is designed according to my workflow of spectral data reduction. However, it is flexible and you can change the order of steps.

1. The software consists of three main parts:
  - The way from 2D images to 1D spectra
  - Image calibration of 2D star (and reference) spectra (dark-/flat-correction)
  - Removal of the sky background
  - Scanning of the single spectra stripes to 1D data
  - Alignment of the spectra (correction of the temperature drift)
2. Wavelength calibration
  - Wavelength calibration with taken reference spectra, or via spectra internal lines or telluric lines
3. Post-processing of the individual spectra or the combined spectra
  - Instrument response correction
  - Optional: removal of the continuum
  - Scaling of the ordinate
  - Cutting to the desired wavelength area
  - Calculation of signal to noise ratio
  - Calculation of the equivalent width



SpectroCalc2 – another way to reduce your spectra

- Finalization of the FITs header data for further calculations and for a valid entry in the BeSS database for Be stars
- Removal of the telluric lines
- Calculation and optional correction of the heliocentric wavelength deviation
- Optional: shift of the spectra by a desired wavelength
- Documentation of the plot (automatic generation of title and legend possible)

The basic way of SpektrCalc2 is to apply all processing steps of parts 1 and 2 to the individual spectra. The big advantage of this method is the high-resolution alignment of the spectra with 1/100 pixel (super-resolution). This is possible because of alignment of the scanned 1D spectra. After the wavelength calibration, you can process each single spectrum or the combined spectra.

## Processing of the exposed 2D spectra into the scanned 1D spectra

The dark-frame and flat-field correction are standard processing and are not further explained in this article.

The sky background correction is of enormous importance in the processing of spectra. This is a subtractive correction, comparable to the dark-frame correction. Without subtracting the sky background, the intensity relationships of absorption and emission lines as well as the curve of the continuum are falsified. SpectroCalc2 automatically calculates the area of the sky background. I recommend checking the result and correcting the area manually if necessary.

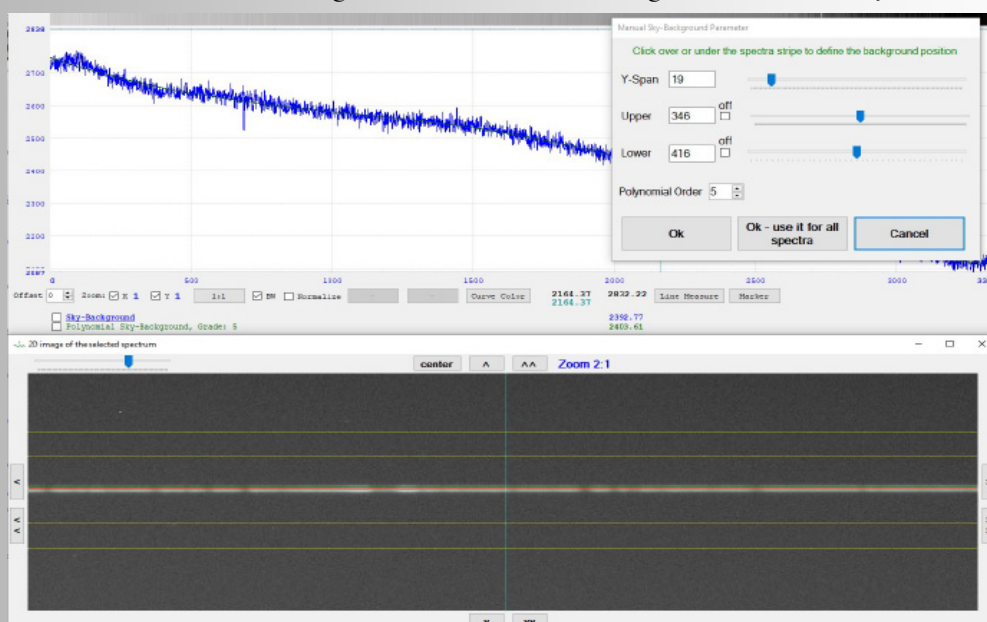
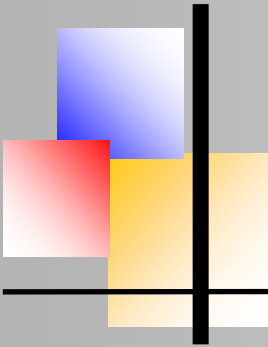


Fig. 1: Sky background correction



## SpectroCalc2 – another way to reduce your spectra

The scanning of the spectra themselves is done automatically. A look at the results of the individual scans is recommended in any case, in order to be able to sort out images with poor quality.

The alignment of the individual spectra is possible with the spectra themselves or with the reference lamp spectra. This process uses a resolution of 1/100 pixel. When using the reference spectra, SpectroCalc2 correlates the spectral images according to the exposure time stamps and corrects them with the same parameters as the reference lamp spectra. The procedure is the same as if you are using the spectra for alignment, but in reverse. In order to get the best results, I recommend always taking a reference lamp image between two star spectra. In this case, you receive precise temperature compensation and thus the narrowest possible absorption or emission lines.

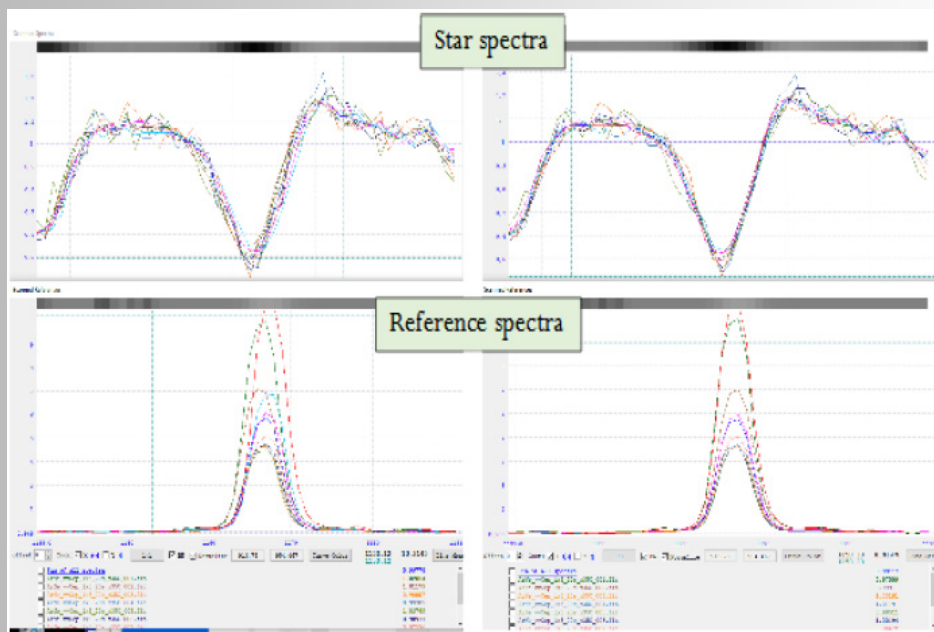
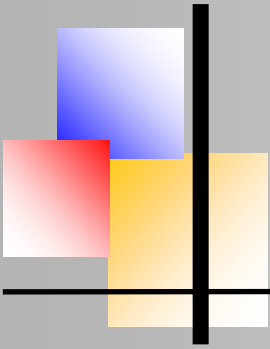


**Fig. 2:** Before and after the spectra alignment

On the left side are the individual spectra (top) and the reference lamp spectra (bottom) before the alignment. On the right side, you see the result of the alignment process.

### Wavelength calibration

Simple text files are used as references for the wavelength calibration. Each user has a different setup, which shows different wavelength areas and resolutions on his camera chip. You should create individual reference files for each setup with the needed calibration lines.



SpectroCalc2 – another way to reduce your spectra

SpectroCalc2 automatically finds the lines in your spectrum. However, you can also choose the lines manually. It is only necessary to assign two lines to the reference wavelengths. After a click on one of your spectral lines, the software calculates the best fit to your references and assigns it automatically. The deviation error, calculated with a previously specified polynomial (curve fitting), is displayed directly. You can immediately estimate incorrectly selected lines or the quality of a manual correction.

After calibration, you can save the result with up to 4-times resolution. Post-processing of the individual spectrum or the combined spectra can now begin.

## **Post-processing of the individual spectrum or the combined spectra**

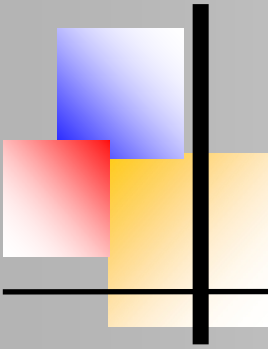
Correction of the instrument response is mandatory when reducing data for a spectrum. The instrument response is the combination of all errors in the instrument chain, such as telescope, spectrograph or camera. The intensity curve over the wavelength is influenced by the instrument response and must be corrected. For this correction, you can use a reference star that you have taken during the same night or you can use a suitable reference star from a public database. If your star is not available in the database, you can use a star within the same spectral and luminosity class.

Spectrocalc2 offers three databases:

- LowRes: a collection of spectra in low resolution
- Miles: the Miles database offers spectra in middle and high resolution
- Elodie: most of the spectra in Elodie are in high resolution. SpectroCalc2 offers only a few examples from this database. It is easy to extend this data base with your desired stars

You can define pre-settings for the calculation of the EW (equivalent width) and the S/N (signal-to-noise ratio). You can also define the range with the mouse or by entering the wavelength range.

In order to be able to examine the radial velocity of an object via absorption or emission lines, you have to correct the influence of the movement of the observer's location on earth. This heliocentric correction takes various parameters and movements into account. It needs to know the location of the observer and of the object, as well as the date and time of the exposure. The correction takes into account the rotation of the earth, the movement around the sun and the influence of the moon.



SpectroCalc2 – another way to reduce your spectra

The intensity of the telluric lines in the spectrum depends on many factors, which can only be described with detailed knowledge of the physics of the earth's atmosphere at the time of the spectrum exposure. In addition to the general correction of the telluric lines, SpectroCalc2 offers the option of correcting each **individual** telluric line separately.

Finally, you can create your own documentation for your spectrum. A mouse click automatically generates the title and a legend with the most important data. However, you can edit this information as well as enter additional text fields in different styles and colours.

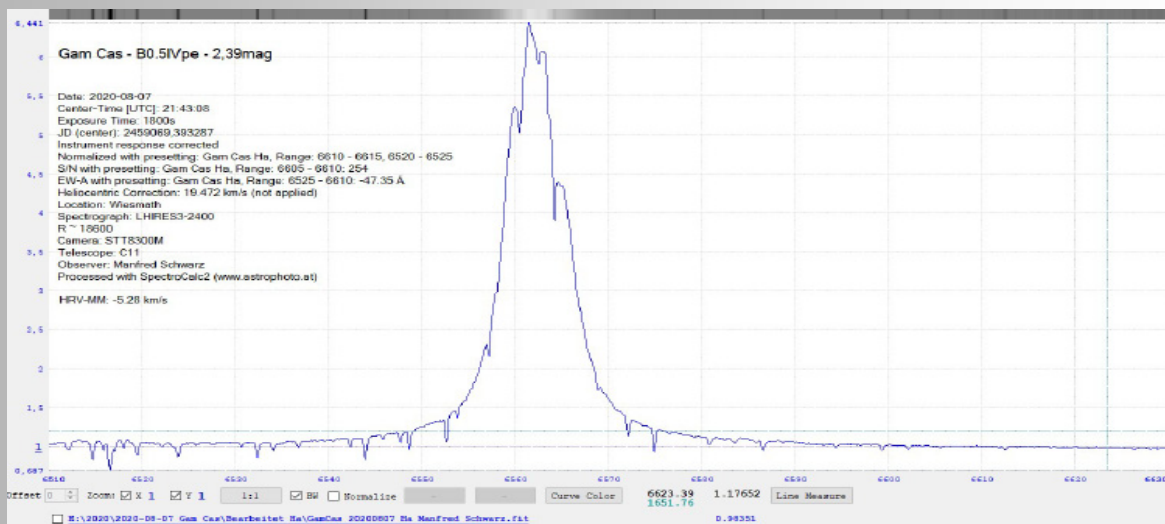


Fig. 3: The final calibrated spectrum of the Be star  $\gamma$  Cassiopeia

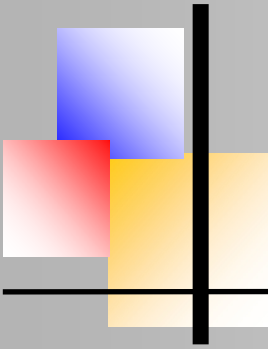
## Necessary resources and references

The software is designed for Windows 7 or higher. It is free of charge and can be downloaded from following website: <http://www.astrophoto.at/spectrocalc2.html>

There you can also find various video tutorials and the manual.

Finally, I would like to thank the following people for their support:

- Ernst Pollmann supported me with his great ideas, intensive tests and constructive criticism
- Roland Bücke supported me with his helpful algorithms for calculating the heliocentric correction
- Hartmut Bornemann supported me with his FITS-IO library
- Sara & Carl Sawicki (Texas) have corrected this article
- All users of SpectroCalc2, who reports bugs and for their great ideas on how to improve this software



## V1405 Cas Nova 2021: About the nature of a multi-maxima nova

Erik Wischnewski, Bundesdeutsche Arbeitsgemeinschaft Veränderliche Sterne e.V. Berlin



### Abstract

**Context:** The Nova V1405 Cas, which erupted on 18 March 2021, showed a pre-maximum phase of almost two months. After the main maximum, over a period of several months, the nova only weakened slightly and showed clear fluctuations in brightness. The aim of this work is to investigate the relationship between brightness and half-width (FWHM) and equivalent width (EW) of the  $H\alpha$  emission line, and from this to infer possible causes for the abnormal behavior of the Nova.

Magnitudes and spectra from online databases were used, the  $H\alpha$  line of the spectra was measured and 2-day normal values were formed in order to establish a temporal comparison. After the main maximum, during the period investigated by JD 2 459 292 to 2 459 305 at intervals of 2–5 weeks, secondary maxima with different characteristics resulted. The maxima of the equivalent width were 6–14 days after the respective brightness maxima. The maxima are interpreted as subsequent outbursts of the nova. Possibly these are subsequent weaker eruptions of the nova or other mechanisms that lead to an increase in density in the envelope.

**Key words** Nova – V1405 Cas – light curves – equivalent width

### Introduction

#### *Characteristics of the Nova*

On 18 March 2021 at 10:10 UT, Yuri Nakamura discovered the Nova Cassiopeiae 2021. The star was already known as a close binary and eclipsing star of the type W Ursae Majoris (EW) under the following names:

CzeV3217

UCAC4 756-077930

PNV J23244760+66111140

Gaia EDR3 2015451512907540480

The equatorial coordinates (J2000.0) are:

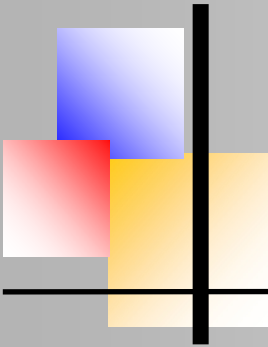
Right ascension = 23h 24m 48s

Declination = + 61° 11' 15"

The distance is  $d = 1693 (+74/-67)$  pc [6].

A period of 0.1883907 days and a brightness of  $V = 15.6$  mag [1] respectively 14.87–14.96 mag [7] are given for the pro-outburst light changes of the star. The orbital period of the double star is 0.376938 days [7].

After the eruption as the nova on 18 March 2021 (RJD 292.3), the star was given the designation V1405 Cas and was classified as a slow nova.



## Aim of the investigation

After the nova initially appeared as a classic He/N nova [11], it did not show the expected decrease in brightness. Instead, the brightness increased again very strongly after a few weeks. The nova remained bright for months and also highly variable. It also turned into a FeII nova. The last nova investigated in more detail by the author was V339 Del (2013), which was a classic FeII nova and for which physical models could also be developed. It is completely different from this nova. On the basis of the brightness measurements as well as the full width at half maximum (FWHM) and equivalent width (EW) of the H $\alpha$  emission line, an attempt should be made to find explanatory approaches.

## Data

Because of the high brightness, the striking behavior of the light curve and the proximity to the open star cluster Messier 52, which is only 0.4 $^{\circ}$  north of the nova, the star was observed photometrically and spectroscopically by amateurs very often. On 18 October 2021, 48 630 brightness information could be downloaded from the *AAVSO International Database (AID)*.

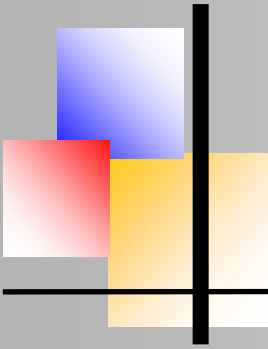
Number of data		
band	total	used
visuell	3147	
CV	32405	32298
CR	3	
U	5	
B	1209	1107
V	5161	4877
R	1165	1130
I	1139	1075
TB	701	614
TG	3307	633
TR	388	385

**Table 1:**

Number of downloaded and used data from the total of 48 630 data sets. *Source: AAVSO International Database, 18 October 2021.*

Only the UBVRI magnitudes should be included in the evaluation. However, because the number was too low, U could not be taken into account. In addition to BVR, the similar colors TB, TG and TR of the RGB channels of a digital camera with Bayer matrix (tricolor) were used and compared with the BVR magnitudes according to John-son-Kron-Cousins.

If in this work the magnitudes R and I are used, then R<sub>c</sub> and I<sub>c</sub> of the Kron-Cousins-System are meant. The CV magnitudes were only loaded for the purpose of comparison with the V magnitudes, but not used for the evaluation of the nova.



V1405 Cas Nova 2021: About the nature of a multi-maxima nova

After checking the reliability of the data, only the number of measurements in the third column of Table 1 were included in the evaluation. The significantly lower number of measurements used in TG can be explained, among other things, by the fact that observers sometimes indicated only 1–2 mmag? as an error. As this is very unlikely even under the most favorable data reduction conditions, these values were not trusted. The individual examination of one observer showed that his values were initially in the main field, but later turned out to be a half magnitude brighter ( $\rightarrow$  Figure 3). This reinforces the suspicion about the usability, so that only about 20% of the TG were used.

Only V and CV magnitudes were considered, the errors of which are below 0.05 mag. For all other color bands, 0.1 mag was used as the margin of error. 71 spectra were used to measure the H $\alpha$  emission line:

Number of spectra	
Source	Number
AVSPE (AAVSO)	57
BAA	8
ARAS	6

**Table 2:** Number of AAVSO, BAA and ARAS spectra used

## Methods

On the one hand, in order to be able to compare the different color bands with one another and to form color indices, normal values were formed. For this purpose, all data were averaged over a progressive 2-day interval. The first interval comprises the measurements from RJD 292.0–294.0 and is assigned to the date RJD 293.0. The next interval then comprises RJD 294.0–296.0 etc. At the same time, this smooths the light curve.

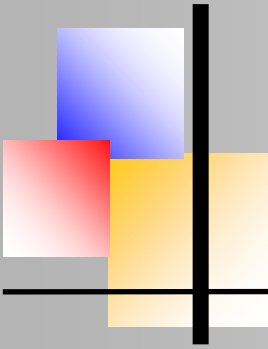
In this work a total of 71 spectra with a spectral resolution of  $R \geq 500$  were evaluated. Of these, 26 have a resolution of  $R \geq 15\,000$ . The equivalent width (EW) and the full width at half maximum (FWHM) of the H $\alpha$  emission line were measured. Further spectra between  $R \geq 200$  and  $R \leq 500$  were unusable for various reasons.

## Results

### *Preliminary examination of the brightness values*

#### *Differences*

Figure 4 to Figure 6 show the differences between the standard magnitudes B, V and R and the tri-color magnitudes TB, TG and TR and Figure 7 contains the difference V–CV. Further information on the comparisons is given in the appendix.



## Color indices

Figure 8 to Figure 13 show the color indices of the standard magnitudes. Notes are also given in the appendix. The diagrams show no peculiarities or systematic trends, with the exception of the color indices (B–R) and (V–R), which have a significant increase at the time of the first maximum of the H $\alpha$  equivalent width. This can still be recognized rudimentarily in the color indices with (V–I), (B–I) and (R–I). This corresponds to expectations, since the H $\alpha$  line lies in the red band. For the sake of completeness, the three color indices were also visualized with the addition of the tricolor magnitudes ( $\rightarrow$  Figure 14 to Figure 16). In Figure 16, in addition to the first maximum, the second maximum at RJD 437 is clearly evident.

## State diagrams

The three-color magnitude diagrams in Figure 17 to Figure 19 do not show any abnormalities and, from the current point of view, do not provide any information on the physics of the nova. The same applies to the two-color index diagram in Figure 20.

## Light curve

Shortly after the discovery, the nova reached its maximum with a visual magnitude of 7.5 mag ( $\approx$ RJD 294). In the period RJD 300–315 it reached an elongated intermediate minimum that fluctuated around 8.0 mag. During this period the spectrum of the nova changed from a He/N nova to a FeII nova. The visual magnitude maximum was  $V = 5.2$  mag on 10/11 May 2021 (RJD  $345.5 \pm 0.5$ ), and thus 53.2 days after the outburst of the nova.

Maxima von V	
Maximum (RJD)	mag
2021-05-11 (346)	5.3
2021-06-07 (373)	6.9
2021-06-17 (383)	6.9
2021-06-29 (395)	6.8
2021-07-27 (423)	6.0
2021-09-09 (467)	6.6
2021-09-21 (479)	6.6

**Table 3:**

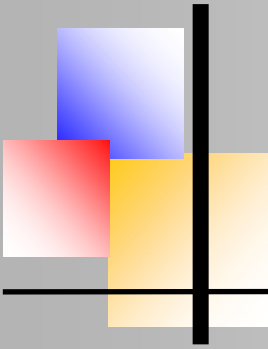
Maxima of the V magnitudes, given in brackets is the RJD based on JD 2 459 000. The column ›mag‹ shows the approximate magnitudes. (Note: Because of the smoothing, the maximum date deviates by about 0.1 mag from the calculated regression value.)

In contrast to a classic nova, in which the main maximum occurs approx. 2–3 days after the pre-maximum, it took almost two months for the Nova Cas 2021 ( $\approx$  52 days).

## H $\alpha$ emission line

### Half width

The full width at half maximum (FWHM) of the H $\alpha$  emission line in Figure 23 was measured consistently in the interval 6510–6616 Å. The measurements of the high-resolution spectra lies



V1405 Cas Nova 2021: About the nature of a multi-maxima nova

in the general stray area of all measurements. In addition to local fluctuations, which in particular have two maxima around RJD 357 and RJD 437, the entire course has an increasing trend, that is, the rate of expansion increases on average over months. This fact is remarkable, which is why it will be discussed in more detail later.

### *Equivalent width*

Two maxima at the equivalent width of the emission line of H $\alpha$  appear particularly clearly in Figure 24. An overview of all minima and maxima is given in Table 4.

Minima and Maxima of EW <sub>H<math>\alpha</math></sub>		
Minimum	Maximum	EW [Å]
2021-05-10 (345)		30
	<b>2021-05-22 (357)</b>	<b>1 700</b>
2021-06-05 (371)		350
	2021-06-13 (379)	940
2021-06-18 (384)		480
	2021-06-24 (390)	870
2021-07-02 (398)		350
	2021-07-09 (405)	870
2021-07-20 (416)		210
	<b>2021-08-10 (437)</b>	<b>2 150</b>
2021-09-18 (476)		70

**Table 4:**

Minima and maxima of the equivalent width of the H $\alpha$  emission line, the RJD is given in brackets based on JD 2 459 000.

### *Intrinsic line flow*

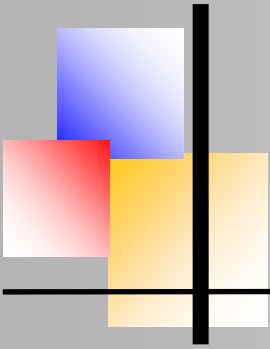
Figure 25 shows the intrinsic H $\alpha$  line flow, calculated on the basis of the visual magnitude V as

$$\frac{-EW_{H\alpha}}{10^{0.4 \cdot V}}$$

Note: The minus sign is only intended to compensate for the negative sign of the equivalent width for emission lines. In this case, intrinsic means that the line flow has been freed (cleared) of fluctuations in the continuum radiation, the continuum being only approximately represented by the photometric magnitude V. The two maxima are also reflected in the intrinsic line flow, although weaker than in the case of the equivalent width. In addition, the R magnitude was used to represent the continuum, in which the maxima are even more clearly developed. This is to be expected since the R magnitude includes the H $\alpha$  lines.

### **Parameters of the star**

The interstellar absorption is calculated from  $A_V = 3.2 \cdot E_{B-V}$ . With  $E_{B-V} = 0.55$  mag [12] the interstellare absorption is  $A_V = 1.76$  mag.



V1405 Cas Nova 2021: About the nature of a multi-maxima nova

A rough calculation with an average extinction in the surrounding area of the sun of 1.0 mag/kpc results in a good agreement of  $AV = 1.7$  mag.

### *Absolute magnitude*

The distance modulus is calculated from  $m - M = 5 \lg d - 5 + A_V$  at the time of the maximum ( $m = 5.2$  mag) and the distance ( $d = 1690$  pc) to  $m - M = 12.90$  mag, corresponding to an absolute magnitude of  $M_V = -7.7$  mag.

### *Luminosity*

The estimation of the luminosity  $L$  is based on the assumption that the bolometric correction  $BC_V$  of the nova is approximately equal to that of the sun, via the absolute visual magnitude  $M_V$ . From

$$\left(\frac{L}{L_{\odot}}\right) = 10^{0.4(M_{V,\odot} - M_V)}$$

with  $M_{V,\text{sun}} = 4.8$  mag, the maximum luminosity of the nova is  $L \approx 90\,000 L_{\text{sun}}$  ( $\rightarrow$  Figure 26).

### *Radius*

The radius can be derived from the Stefan-Boltzmann law:

$$\frac{L}{L_{\odot}} = \left(\frac{R}{R_{\odot}}\right)^2 \cdot \left(\frac{T}{T_{\odot}}\right)^4$$

With a photospherical envelope temperature of the nova of  $T = 9000$  K [16] and the effective temperature of the sun of  $T_{\text{eff}} = 5778$  K, a maximum radius of  $R \approx 125 R_{\text{sun}}$  is calculated ( $\rightarrow$  Figure 27).

### *Distance of the double star*

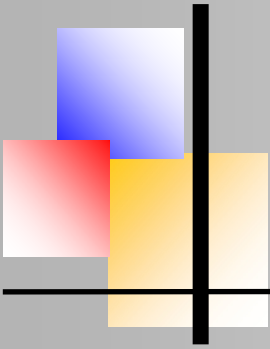
From the Kepler relationship

$$\left(\frac{a}{AU}\right)^3 = \left(\frac{M_1 + M_2}{M_{\odot}}\right) \cdot \left(\frac{U}{\text{year}}\right)^2$$

with  $U = 0.377$  d  $\approx 0.001$  years [7] and the assumed masses  $M_1 = 1 M_{\text{sun}}$  and  $M_2 = 2 M_{\text{sun}}$  a major semiaxis of  $a = 0.0147$  AE  $\approx 3.2 R_{\text{sun}}$  results. The nova envelope therefore covered the entire binary system.

### **Discussion**

On 3 April 2021 (RJD 308) the nova showed a helium spectrum, on 19 April 2021 (RJD 324) the iron lines were already clearly in the foreground [13]. As a result, the initial He/N nova



V1405 Cas Nova 2021: About the nature of a multi-maxima nova

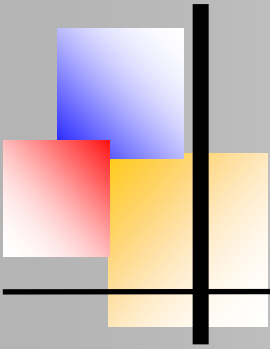
must have mutated into an Fe II nova in the period from 5 April 2021 to 20 April 2021 (RJD 310– 325). This is exactly the broad minimum between the premaximum and maximum of the brightness ( $\rightarrow$  Figure 21). There seems to be a connection between the course of brightness (light curve) and the change in the nova spectral type. On 8 May 2021 the spectrum at the maximum brightness corresponded to a textbook Fe II nova [14].

Highly ionized emission lines in the spectra indicate that the nova photosphere has not expanded enough to cool itself down [11]. The spectrum looks very similar to that of the nova V339 Del. The complete absence of forbidden metallic emission lines suggests that even 15 weeks after the eruption and 55 days after maximum brightness ( $\approx$  RJD 400) the density of the ejection is high enough to prevent the formation of these lines [15]. After a first outburst with an increase in brightness of  $\approx 8.1$  mag (= pre-maximum), a second one followed with a further increase in brightness of  $\approx 2.3$  mag (= main maximum) and then further weaker increases. A closer look at the temporal development of the brightness on the one hand and the equivalent width on the other hand shows that the EW maxima occurred 6-14 days after the respective brightness maxima.

Several mechanisms are conceivable as the cause, but in the opinion of the author they must all result in an increase in the matter density of the shell. It is not yet possible to deduce from these data whether these occurred through eruptive eruptions or in a more gentle way. As shown in the section 'Intrinsic line flow', an increase in the equivalent width can also be caused by an increase in the continuum radiation. The timely increase in the V magnitude and the equivalent width EW indicate precisely this fact. The intrinsic line flow is only partially corrected for continuum, as Figure 25 shows, where the maxima are still present. The high matter densities of the photosphere (shell) mentioned in [11] and [15] can be explained by the additional, more or less strong material replenishment, which can be determined both in the light curve and in the equivalent width.

### **Expansion velocity**

In a classic nova, the matter of the eruption is accelerated by the radiation pressure. Nevertheless, one observes a decreasing rate of expansion over time, because it relates to the photosphere. The photosphere, however, migrates inward over time, because the shell becomes thinner and thinner due to the lack of material supply. This allows us to see deeper and deeper layers of the envelope, which has not yet been accelerated that much [10]. In the case of Nova Cas 2021, however, a steadily increasing (average) rate of expansion can be observed in the first 7 months. This can only be explained if matter is constantly being supplied over the entire period. Apparently this does not happen continuously, but in bursts, as the maxima in the brightness and the flow of lines show.



## Conclusions

V1405 Cas initially presented itself as a He/N nova in the pre-maximum and then mutated into a classic FeII nova also? during the pre-maximum phase.

This pre-maximum phase, which usually lasted only a few days, lasted for more than seven weeks. Detailed spectral studies will be necessary to understand the exact process during this time.

After the main maximum, the nova not only remained relatively bright for months, but also regularly showed outburst-like secondary maxima at intervals of 2–5 weeks. These maxima first appeared in the visual continuum and 1–2 weeks later in the H $\alpha$  equivalent width. The author suspects that a similar process is responsible for this as well as for the long-lasting pre-maximum phase. There is still a need to explain the time lag between the continuum and line maximum.

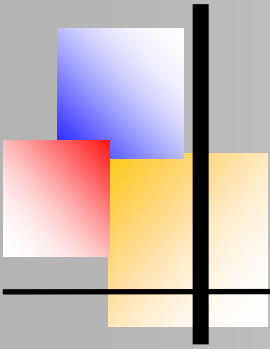
Since the nova outburst is caused by the accreted matter from the companion (donor), it cannot be completely ruled out that the cause of the special behavior of this nova lies in this accretion flow. In the case of a recurring nova of the type NR it takes 10–10,000 years until the next eruption; here it is only a few weeks. So there has to be a crucial difference between the two re-excitation mechanisms, or it is simply a completely different process.

In this investigation, the light curve and the flow of lines were compared with each other for the first time and the nova was described as a quasi multi-maxima nova. Building on this, further data must now be collected as already described.

## Acknowledgements

This research made use of the SIMBAD database and of the VizieR catalogue access tool, operated at CDS, Strasbourg, France, and the International Variable Star Index (VSX) database, operated at AAVSO, Cambridge, Massachusetts, USA. The author acknowledges with thanks the variable star observations from the AAVSO International Database contributed by observers worldwide and used in this research [2].

The author thankfully acknowledges further the spectra from the AAVSO Database AVSPEC [3], ARAS Spectral Database [4] and BAA Spectroscopy Database [5] contributed by Hugh Allen, Mariusz Bayer, Christophe Boussin, David Boyd, John Briol, Erik Bryssinck, Mario Clemens, Scott Donnell, James Foster, Joan Guarro Fló, Peter Somogyi and Tim Stone, and used in this research. The author would like to thank Tom Fields for providing and supporting the RSpec software [8].



# BAV MAGAZINE SPECTROSCOPY



V1405 Cas Nova 2021: About the nature of a multi-maxima nova

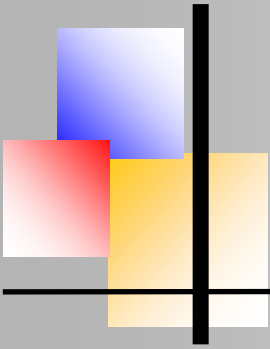
## References

- International Variable Star Index (VSX), operated at AAVSO: [www.aavso.org/vsx](http://www.aavso.org/vsx)
- AAVSO International Database (AID): [www.aavso.org/data-download](http://www.aavso.org/data-download)
- AAVSO Database of Spectra (AVSPEC): [app.aavso.org/avspec/search](http://app.aavso.org/avspec/search)
- ARAS Spectral Database: [articles.adsabs.harvard.edu/pdf/2019CoSka..49..217,](http://articles.adsabs.harvard.edu/pdf/2019CoSka..49..217,)  
[www.astrosurf.com/aras/Aras\\_DataBase/DataBase.htm](http://www.astrosurf.com/aras/Aras_DataBase/DataBase.htm)
- BAA Spectroscopy Database: [britastro.org/specdb/index.php](http://britastro.org/specdb/index.php)
- Bailer-Jones, Coryn et al.: *Abschätzen von Entfernungen von Parallaxen. V: Geometrische und photogeometrische Entfernungen zu 1.47 Milliarden Sternen in Gaia Early Data Release 3.* *Astronomical Journal* 161 (2021), 147. [gaia.ari.uni-heidelberg.de/tap.html](http://gaia.ari.uni-heidelberg.de/tap.html)
- CzeV, The Czech Variable Star Catalogue: [var2.astro.cz/czev.php](http://var2.astro.cz/czev.php)
- Fields, Tom: Software RSpec, [www.rspec-astro.com](http://www.rspec-astro.com)
- Wischniewski, Erik: *Astronomical Bulletin No. 22*, [www.astronomie-buch.de](http://www.astronomie-buch.de)
- Hachisu, Izumi and Mariko Kato: *The UBV Color Evolution of Classical Novae.* arXiv:1401.7113v1 (2014)
- Taguchi, Kenta et al.: ATel #14472, 19. 03. 2021
- Munari, Ulisse et al.: ATel #14476, 19. 03. 2021
- [13] Shore, Steven N. et al.: ATel #14577, 26. 04. 2021
- [14] Munari, Ulisse et al.: ATel #14614, 08. 05. 2021
- [15] Gehrz, Robert D. et al.: ATel #14794, 17. 07. 2021
- [16] Friedjung, M. and Hilmar W. Duerbeck: *Models of Classical Recurrent Novae.* *NASSP* (1993), 371–412

## Appendix

The appendix contains all diagrams and figures mentioned within the text (next page).





V1405 Cas Nova 2021: About the nature of a multi-maxima nova

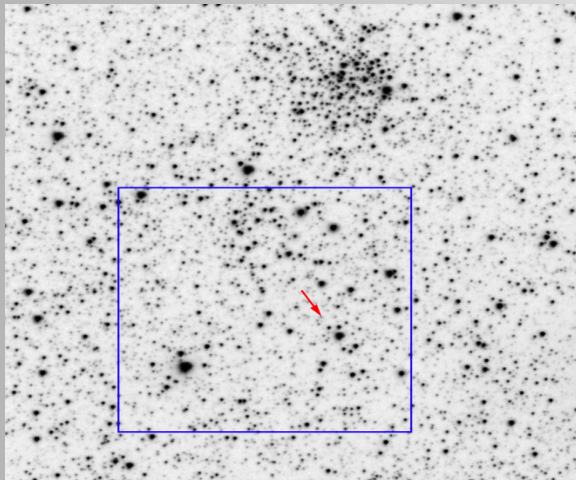


**Fig. 1:** Area map with M 52 from 2013-09-29. The progenitor of the nova is marked (red arrow). The blue frame indicates the approximate section of Figure 2.

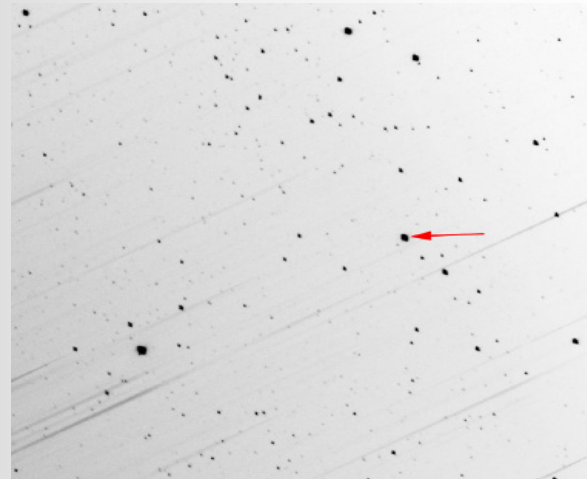


**Fig. 2:** Part of the spectral recording with clearly recognizable nova (red arrow).

### *Plausibility check*

The observations were subjected to a plausibility check before they were used for evaluation.

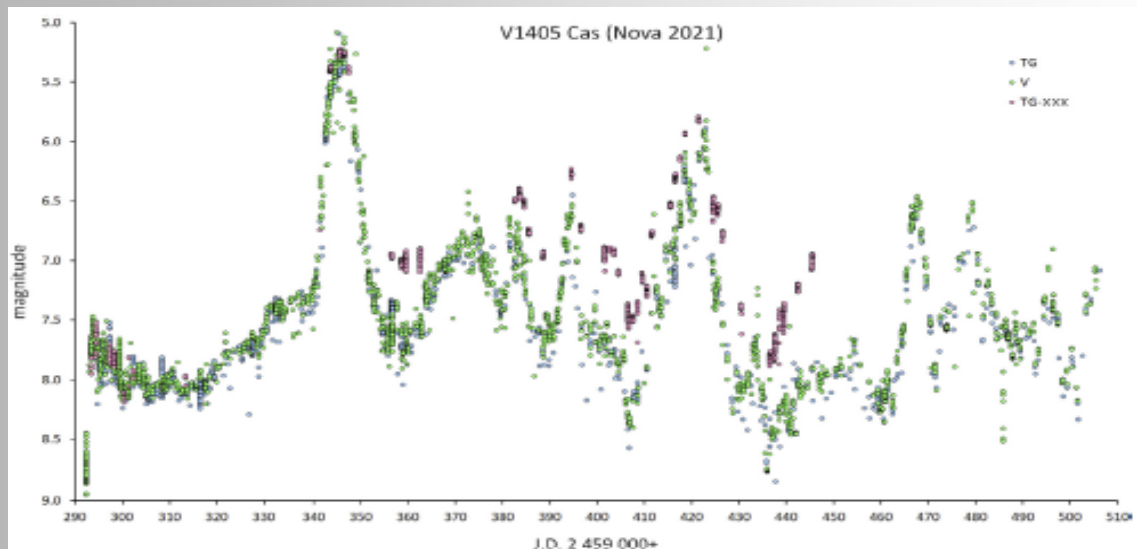
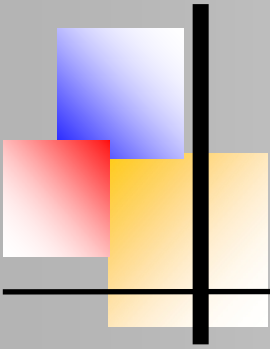


**Fig. 3:** Example of the measurements in the TG band of the (anonymized) observer XXX. The clear deviations in the period JD 2 459 350 to JD 2 459 450 led, among other things, to not taking this data into account (for the time being). The observer has been informed.



V1405 Cas Nova 2021: About the nature of a multi-maxima nova

### *Comparison of tricolor to standard magnitudes*

Since the data of the bands TB, TG and TR of a tricolor digital camera with Bayer matrix are typically not calibrated by the observers to the photometric standard system according to Johnson-Kron-Cousins, it was necessary to check how these values relate to the standard magnitudes B, V and R behave. The differences are considered. For further evaluations, the standard and tricolor magnitudes are used together and as  $B'=[B, TB]$ ,  $V'=[V, TG]$ ,  $R'=[R, TR]$  designated.

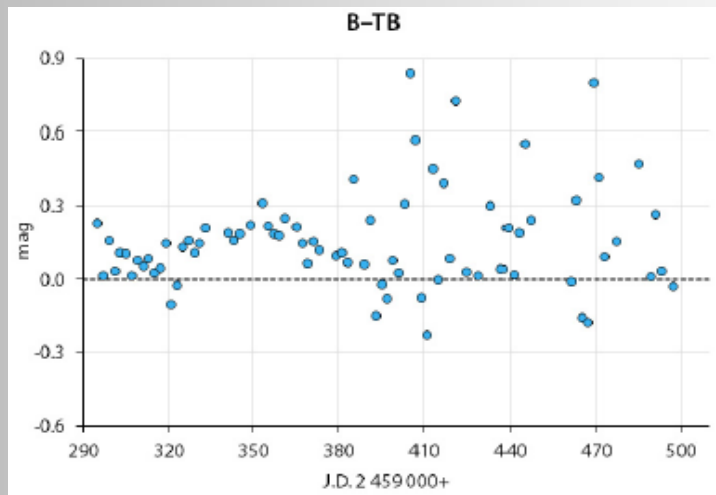


**Fig. 4:** Difference between the Johnson magnitude B and the tricolor magnitude TB. It is noticeable that the TB magnitudes are predominantly brighter than the B magnitudes and also scatter strongly.

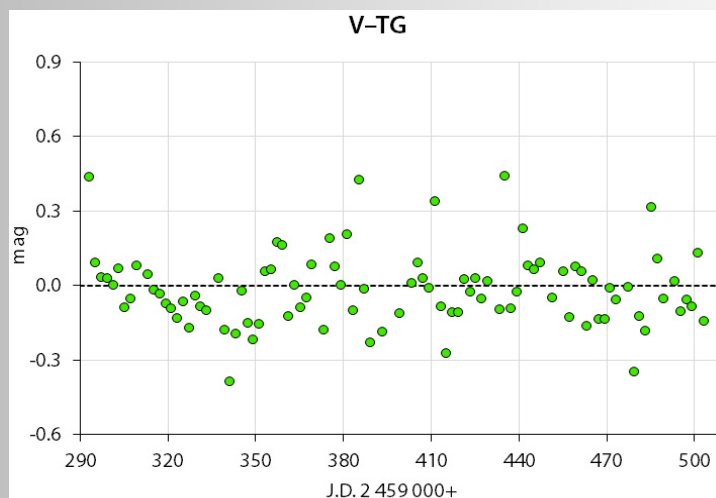
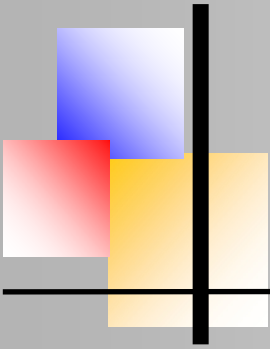


**Fig. 5:** Difference between the Johnson magnitude V and the tricolor magnitude TG (G = green). The TG magnitudes are at the same level as the V magnitudes, but with a clear spread.



V1405 Cas Nova 2021: About the nature of a multi-maxima nova

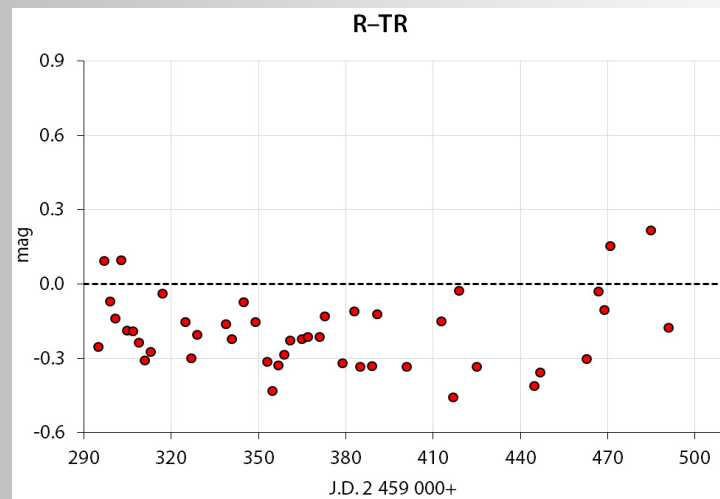


**Fig. 6:** Difference between the Johnson-Kron-Cousins magnitude R (RC) and the tricolor magnitude TR. It is noticeable that the TR magnitudes are predominantly darker than the RC magnitudes and also scatter significantly.

### *Compare V to CV*

Monochromatic CCD astronomical cameras, which only use a UV/IR blocking filter, record the entire spectral range from blue to red (referred to as *clear*). If the V magnitudes are used for the reference stars, this brightness is referred to as CV. A comparison with magnitudes, which were also recorded with a Johnson V filter, shows a clear deviation with a large.

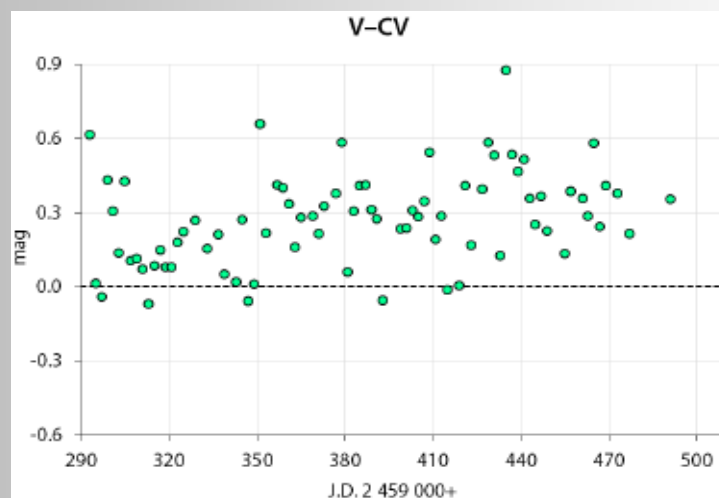
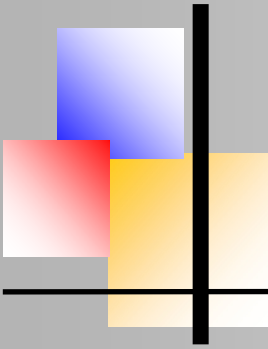


**Fig. 7:** Difference between the Johnson magnitude V and the unfiltered magnitude CV. The CV magnitudes are generally brighter than the V magnitudes and also scatter very strongly.



# BAV MAGAZINE SPECTROSCOPY



V1405 Cas Nova 2021: About the nature of a multi-maxima nova

## *Color indices of the standard magnitudes*

In addition to the light curve in a certain color band, the light curves of the color indices, i. e. the difference between two color bands, are also of interest. A physical interpretation is not yet possible in the case of the nova, only the color indices B-R and V-R reflect the first maximum of the equivalent width of the H $\alpha$  line.

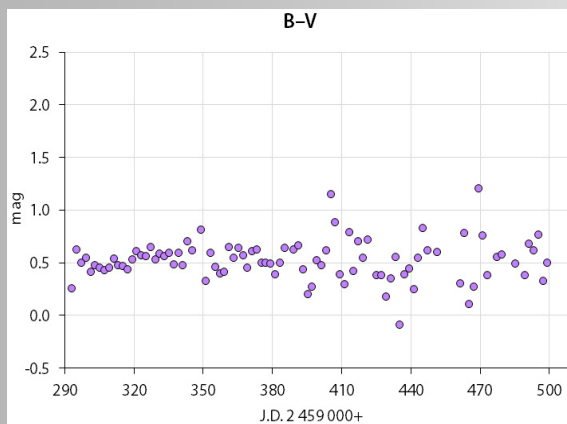


**Fig. 8:** Color index B-V of the normal values over 2 days

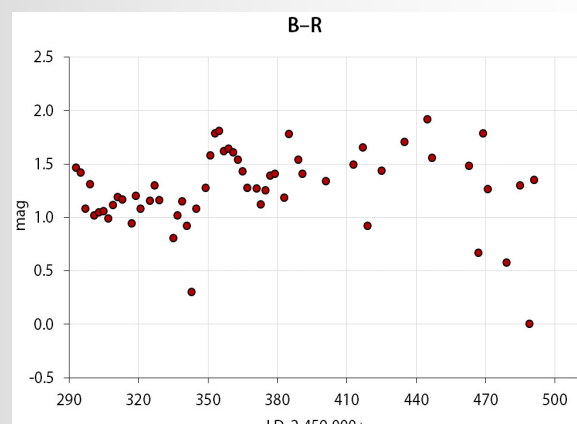


**Fig. 9:** Color index B-R of the normal values over 2 days

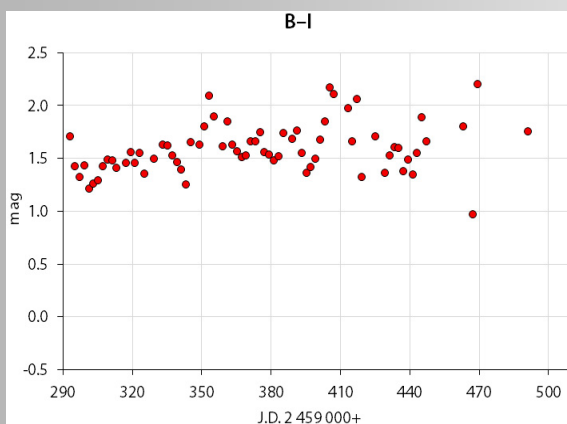


**Fig. 10:** Color index B-I of the normal values over 2 days.

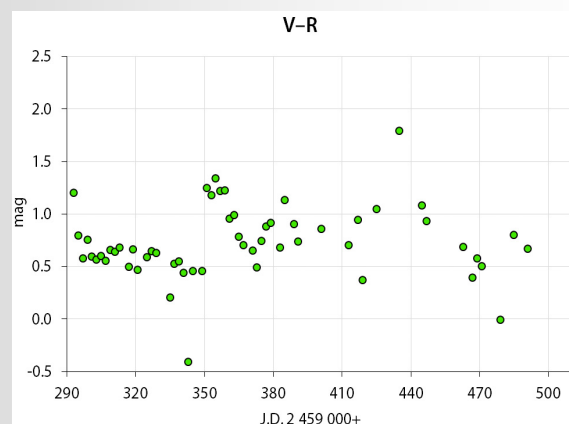
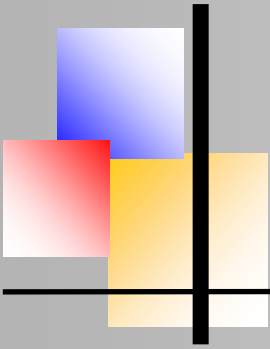


**Fig. 11:** Color index V-R of the normal values over 2 days.



V1405 Cas Nova 2021: About the nature of a multi-maxima nova

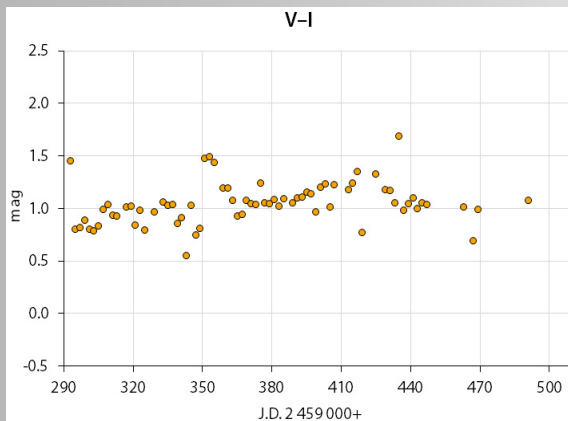


**Fig. 12:** Color index V-I of the normal values over 2 days.

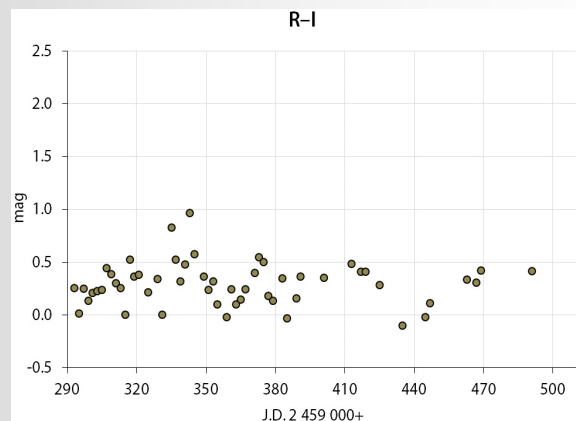


**Fig. 13:** Color index R-I of the normal values over 2 days.

### *Color indices of the combined magnitudes*

The inclusion of the tricolor measurements in the generation of the normal values reduced the scatter of the color indices slightly.

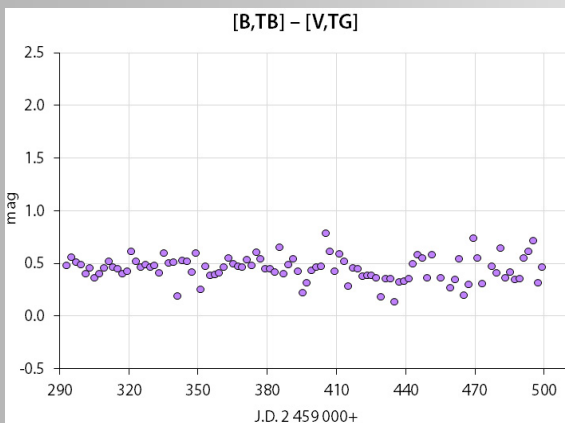


**Fig. 14:** Color index (B'-V') of the normal values over 2 days

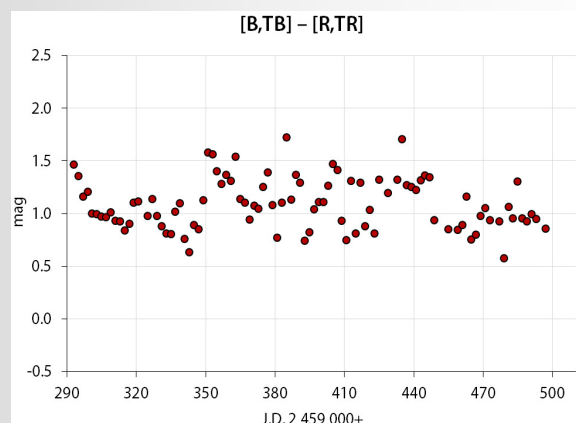
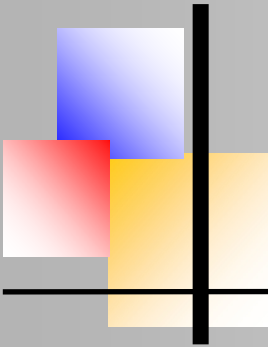


**Fig. 15:** Color index (B'-R') of the normal values over 2 days



# BAV MAGAZINE SPECTROSCOPY



V1405 Cas Nova 2021: About the nature of a multi-maxima nova

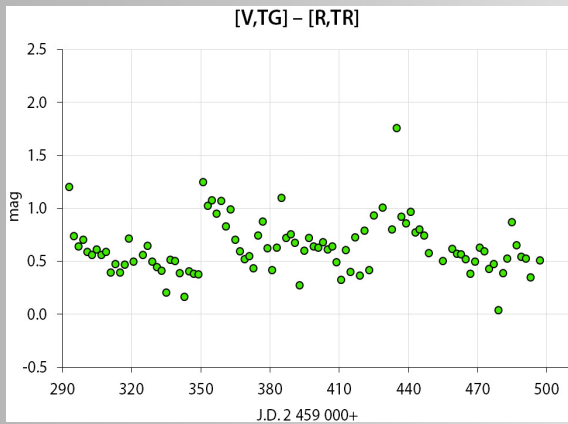


**Fig. 16:** Color index ( $V^I - R^I$ ) of the normal values over 2 days

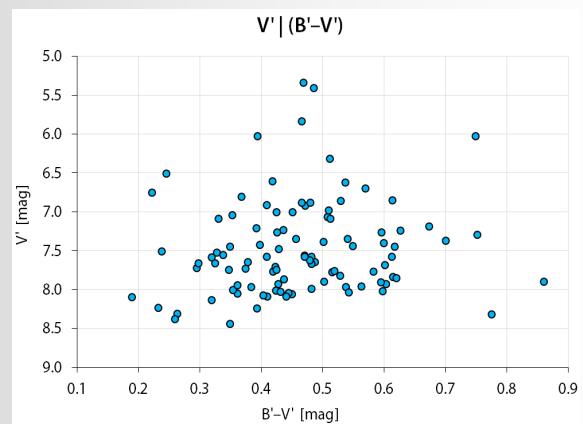


**Fig. 17:** Visual magnitude  $V^I$  versus the color index ( $B^I - V^I$ ).

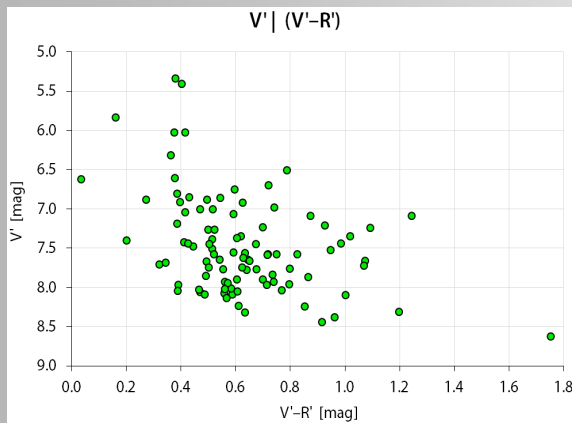


**Fig. 18:** Visual magnitude  $V^I$  versus the color index ( $V^I - R^I$ ).

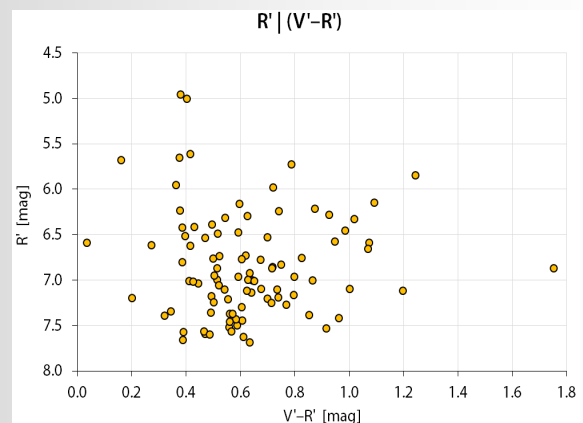
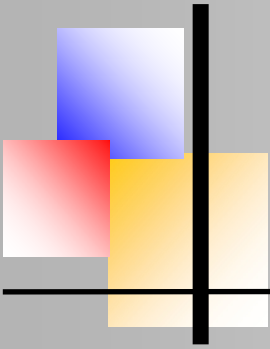


**Fig. 19** Red magnitude  $R^I$  versus the color index ( $V^I - R^I$ ).





# BAV MAGAZINE SPECTROSCOPY



V1405 Cas Nova 2021: About the nature of a multi-maxima nova

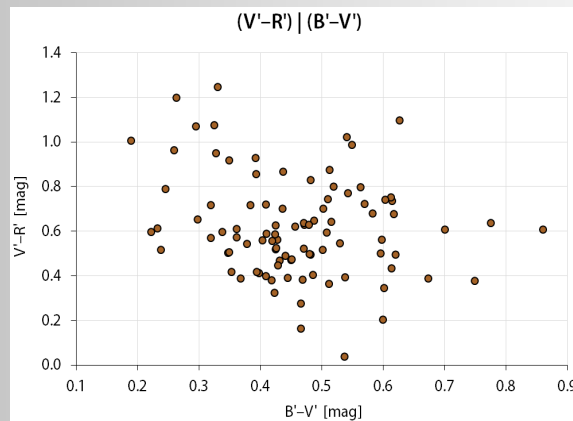


**Fig. 20:** Two-color index diagram of the color indices ( $V'-R'$ )

### *Light curve, $H\alpha$ emission line, luminosity and radius*

The discussion of the following diagrams takes place in the main part of this paper.

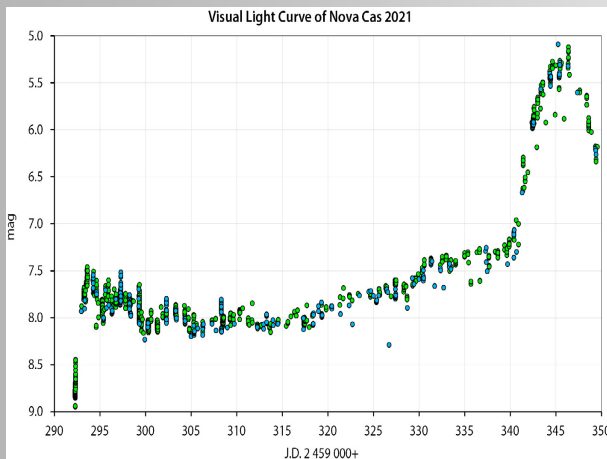


**Fig. 21:**

Individual observations of the first two months in the bands V (green dots) and TG (blue dots).

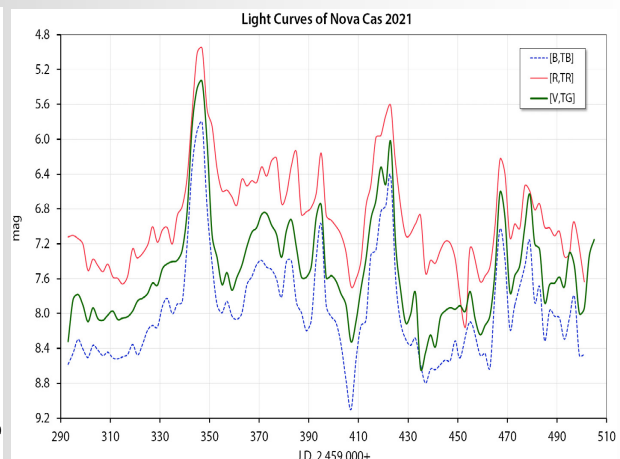
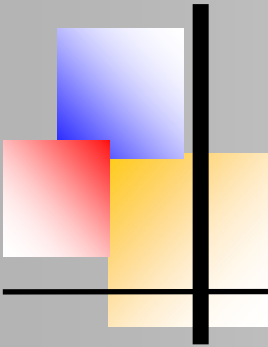


**Fig. 22:**

Light curves of the 2-day normal values in the three color ranges blue, green and red, each using the standard magnitudes B, V and R as well as the tricolor magnitudes TB, TG and TR ( $= B', V', R'$ ).



## V1405 Cas Nova 2021: About the nature of a multi-maxima nova

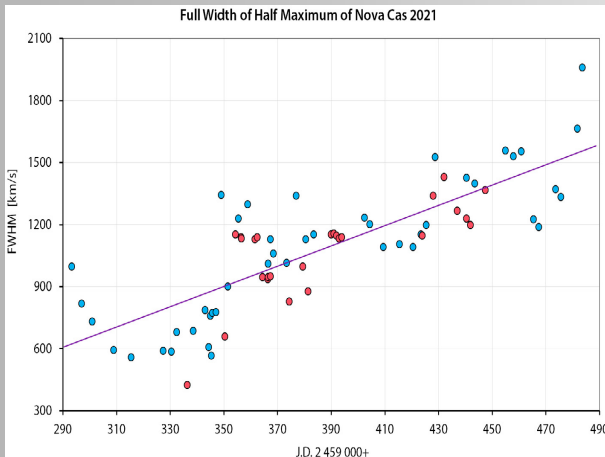


**Fig. 23:**

Full width at half maximum (FWHM) of the  $H\alpha$  line, given as speed in km/s. The blue dots indicate spectra with  $R = 500\text{--}1500$ , the red dots represent spectra with  $R \geq 15000$ . The expansion rate increases steadily on average, superimposed by temporary fluctuations

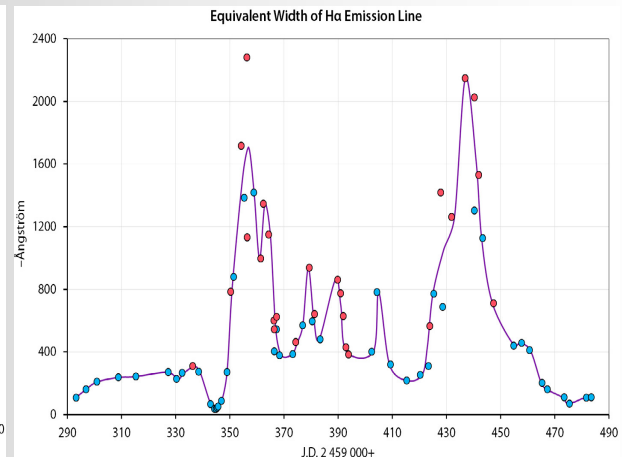


**Fig. 24:**

Equivalent width (EW) of the  $H\alpha$  line, one (averaged) value per 2-day interval, given in Angstrom. The blue dots indicate spectra with  $R = 500\text{--}1500$ , the red dots represent spectra with  $R \geq 15000$ . Two dots were averaged for the purple curve.

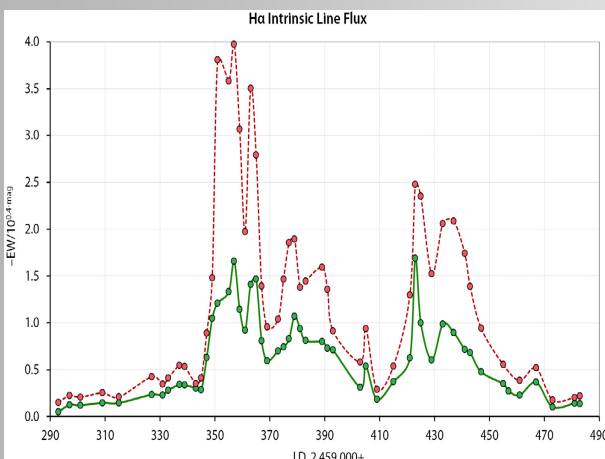


**Fig. 25:**

Intrinsic line flow of the  $H\alpha$  line, one (averaged) value per 2-day interval, using the magnitudes  $V'$  (green dots) and  $R'$  (red dots).

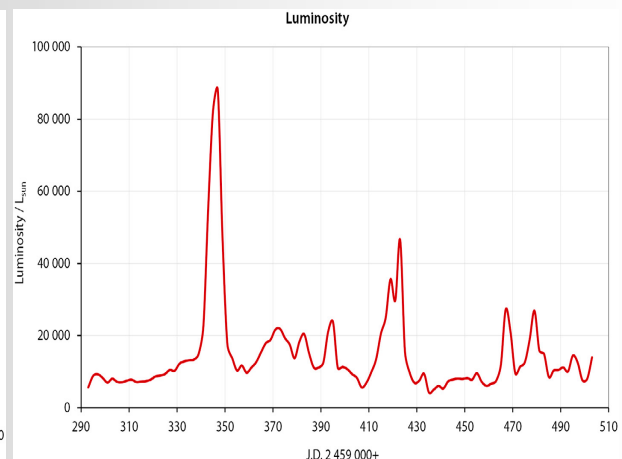
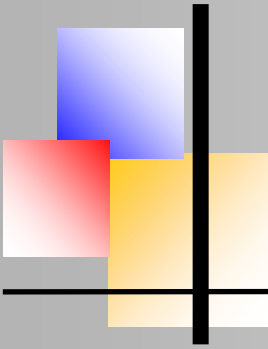


**Fig. 26:**

Luminosity in units of solar luminosity.



V1405 Cas Nova 2021: About the nature of a multi-maxima nova

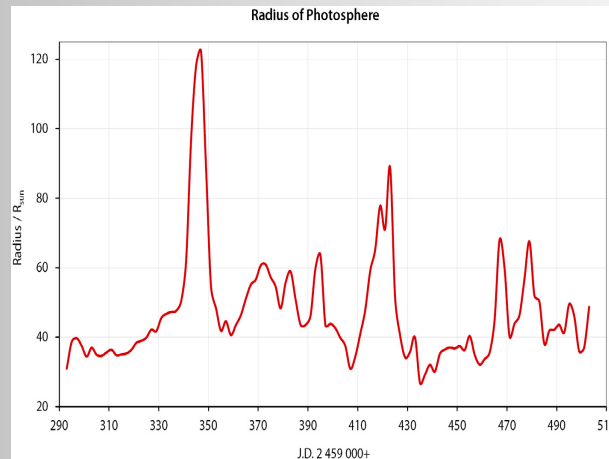


**Fig. 27:**  
Radius of the photosphere of the shell in  
units of the solar radius

---

## Spectroscopy of Stellar Flares

Robert K. Buchheim

[Bob@RKBuchheim.org](mailto:Bob@RKBuchheim.org)

Forrest Sims, Jack Martin, Albert Stiewing, Gary Walker

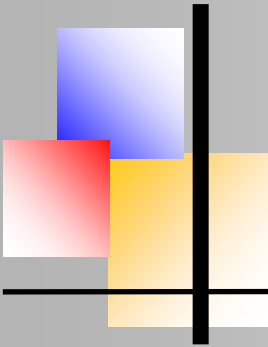


### Abstract

Small telescopes with modest spectrographs can observe and record the signature of stellar flares, with good sensitivity and time-resolution. This may be a fruitful addition to the observational record on stellar flare activity. We might be able to significantly increase the number of well-observed flares; provide a spectroscopic record of the flares; characterize the out-of-flare stellar activity; and illustrate the relationship between the photometric and spectroscopic signatures of flares.

### Motivation

Once upon a time, I recall reading about “flare stars”, whose brightness can jump dramatically in just a few minutes, before fading back to normal. I even spent a couple of hours staring at one



through the eyepiece of my 6-inch Newtonian, but to no avail. Flares occur randomly, so there is only a small chance of seeing one in a two-hour observing session; and most of the time they give only a small delta-magnitude. So, they were tucked away in the back of my mind, as something to return to, someday. Now, 30 years later, “someday” arrived.

A presentation at the 237th AAS meeting [Notsu et al, 2021] about spectral-line changes during a stellar flare caught my interest because it noted that “more observations are needed”. This project seemed to be in the sweet spot for amateur spectroscopists. It is difficult for professionals to schedule the necessary long observing runs, but we amateurs can freely devote our equipment and time to whatever interests us, regardless of the low probability of success. It re-kindled the idea of seeing a stellar flare for myself.

The initial concept of this project was to pick a target and stare at with a spectrograph, all night for a few nights, to see what could be seen.

### Target: AD Leo

After a brief literature search of candidate flare-stars, I selected AD Leo as a target. It is bright ( $V \approx 9.4$ ), it was well-placed for observing early in the year, and it is known to be a particularly active flare star when observed photometrically and spectroscopically.

The star’s spectrum is that of a typical early-M dwarf, except that it always shows strong emission in the Balmer lines, and Ca II (K), as shown in Fig. 1.

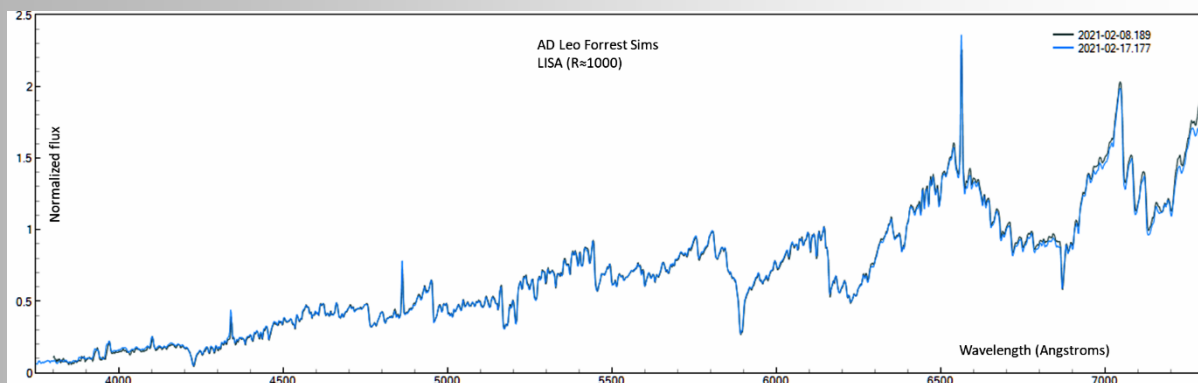
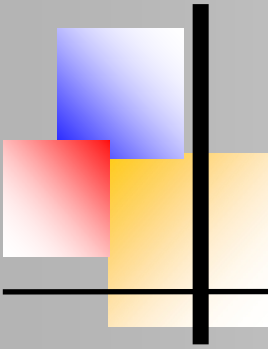


**Fig. 1:** AD Leo’s spectrum displays strong emission in the Balmer and Ca II (K) lines at all times.

In a bit of good fortune, after just a couple of all-night observing sessions I was rewarded with an event in which the Balmer lines all strengthened simultaneously, and then decayed back to their normal “quiescent” level, as shown in Fig.2:



# BAV MAGAZINE SPECTROSCOPY



Spectroscopy of Stellar Flares

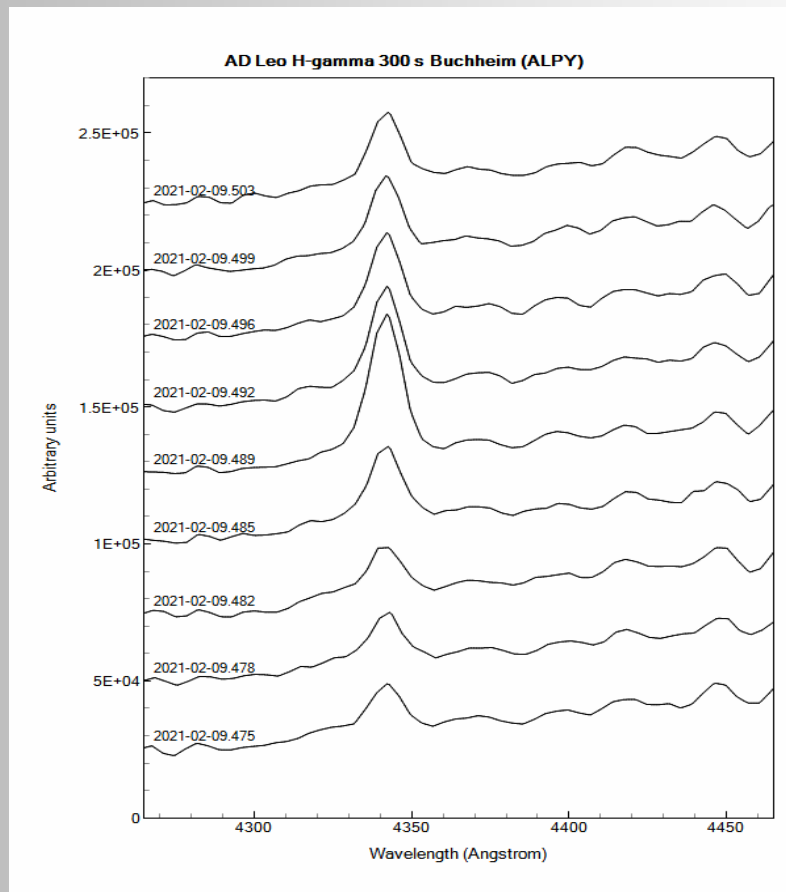
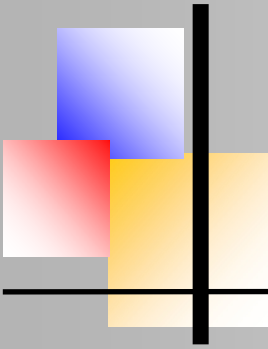


**Fig. 2:** This stacked plot of spectra shows the rise and fall of the H $\gamma$  emission line during a flare on AD Leo. Time runs from the bottom to the top. This series of spectra spans about 40 minutes.

This turned out to be the stereotypical signature of a flare. Soon, several of my friends – all amateur astronomers – joined the search for flares.

## What we did

Individual observers conducted long runs of time-series spectra as permitted by their personal schedules and weather. In total, between February and April 2021, the team accumulated about 200 hours of spectroscopic observations, comprising over 2400 individual spectra. Low-resolution spectra (Shelyak ALPY,  $R \approx 500$  and Shelyak LISA,  $R \approx 1000$ ) were generally made using continuous series of 300s exposures. High-resolution (Shelyak LHIRES) used either 300s or 600s exposures, several different gratings (hence different spectral resolution) and were aimed at either the H-alpha or H-beta lines. All observations were made with small telescopes



(ranging from 14- to 16-inch aperture) from suburban sites. Most observing runs spanned the whole time that the target was observable (over 8 hours/night in February, dropping to about 5 hours/night in April). Long observing sessions are needed for two reasons: first, we needed to accumulate quite a few hours in order to have a chance of capturing a flare; and second, the duration of the flares in the optical spectra ranges from a few minutes to an hour or longer. An hour-long event would be difficult to recognize if the observing run were less than two or three hours long. Calibration lamp images were taken at the beginning and end of each run, and usually also mid-way through the run (at meridian flip). In the case of the low-resolution spectra, “Reference Star” observations for correction of instrumental response and atmospheric extinction were also taken on most nights. Raw spectrum images, along with bias and dark frames, flat frames, and Calibration lamp exposures were processed using ISIS software in the usual way. We took advantage of two features of ISIS that were new to most of us:

(1) We selected “Erase intermediate files” = “No”. This tells ISIS to create and report a spectrum for each individual image, rather than only reporting a spectrum based on combining all images.

(2) We took advantage of the “Auto atmosphere” feature in ISIS, which automatically adjusts the Atmospheric Response correction for the air mass of each image.

This results in a time-series set of fully processed spectral profiles, each one displaying relative flux vs wavelength.

### What we saw

Fig. 3 shows the spectral signature of a pretty big flare, in a continuous sequence of 300 sec images using an ALPY spectrograph.

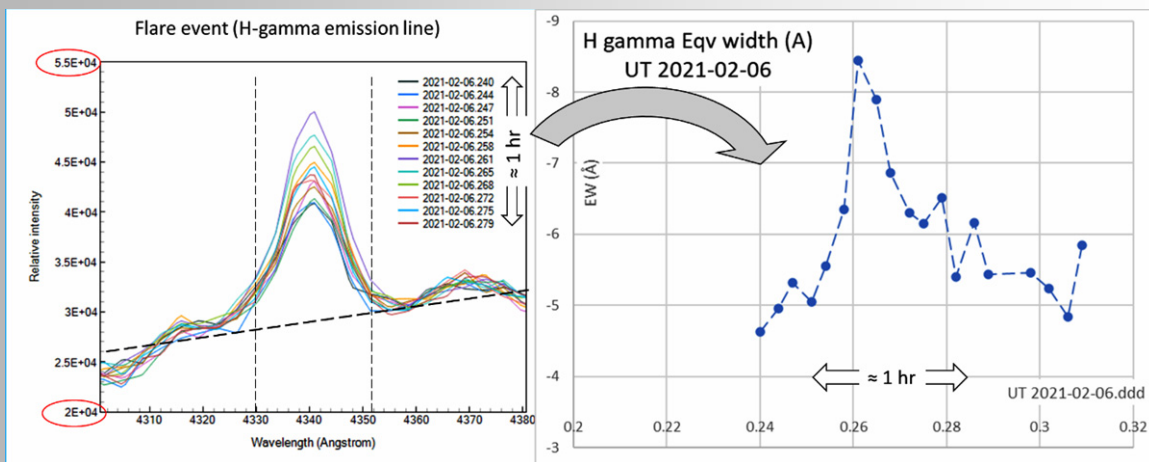
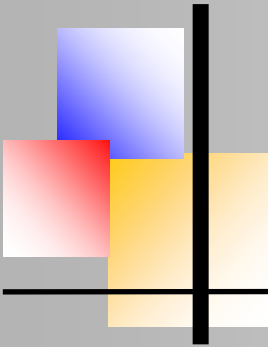


**Fig. 3:** A typical time-series set of spectra (left panel, centered on the H $\gamma$  line), and the calculated Equivalent Width vs. time (right panel). Over the course of an hour, the emission line strengthens significantly, then fades back to its quiescent level.



# BAV MAGAZINE SPECTROSCOPY



## Spectroscopy of Stellar Flares

The 300-sec observing cadence seemed to be a good balance between time-resolution and SNR for this star. Since low-resolution spectra (ALPY and LISA) show the entire optical band, we could follow the evolution of all the Balmer lines. In all of the flares that we recorded, the Balmer lines strengthened and returned to quiescence simultaneously, with no apparent time-delay between them, as shown in Figure 4. There is a noticeable difference between the amount of EW change, from line to line. We saw a consistent pattern that H $\gamma$  displayed the most obvious flare-signal, followed by H $\delta$  and H $\beta$ , and with H $\alpha$  showing a relatively weak increase in EW during a flare.

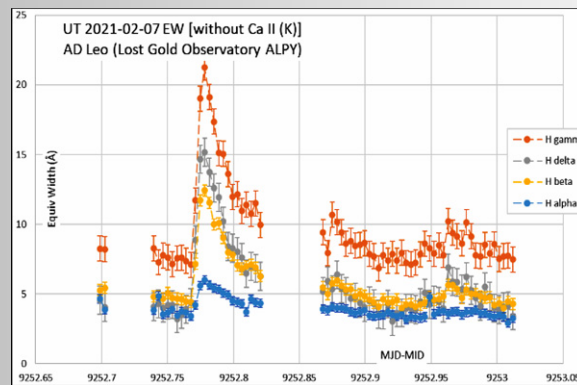


**Fig. 4:** Evolution of Balmer lines H $\gamma$ , H $\delta$ , H $\beta$ , and H $\alpha$  during a flare on AD Leo. The gap in the middle of the plot is the time devoted to “meridian flip”, calibration lamp, and reference star spectra. The “Fast Rise, Exponential Decay” profile shown in this flare is typical, but not universal.

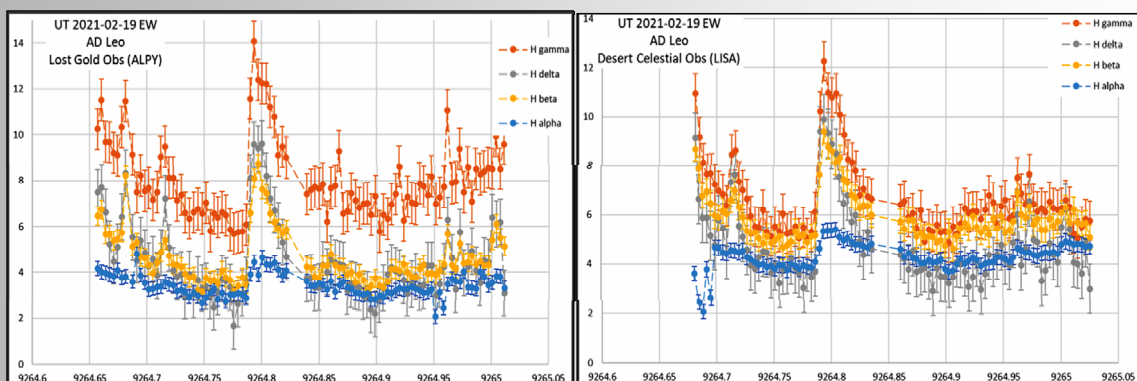
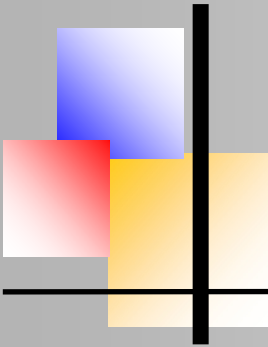


**Fig. 5:** This flare was observed from two observatories, separated by about 20 miles, using different spectrograph models and different telescope types.



The fact that all the Balmer lines rise and fall together, with a recognizable pattern, seemed like good subjective evidence that we were seeing something “real” from the star. A couple of times, two of us saw the same flare at the same time, from widely separated observatories using different instruments, and captured virtually identical plots of EW vs. time, as shown in Fig. 5. That is pretty convincing evidence that what we are seeing is a real signal from the star, not a “noise” or local artifact.

Our goal in experimenting with high-resolution spectra was to investigate the feasibility of detecting and characterizing line-profile changes during flare events. This obviously presents a difficult trade-off, to achieve acceptable accuracy in flux (SNR) while also providing acceptable time-resolution. There may also be a less-obvious tradeoff in the decision of which emission line to monitor.

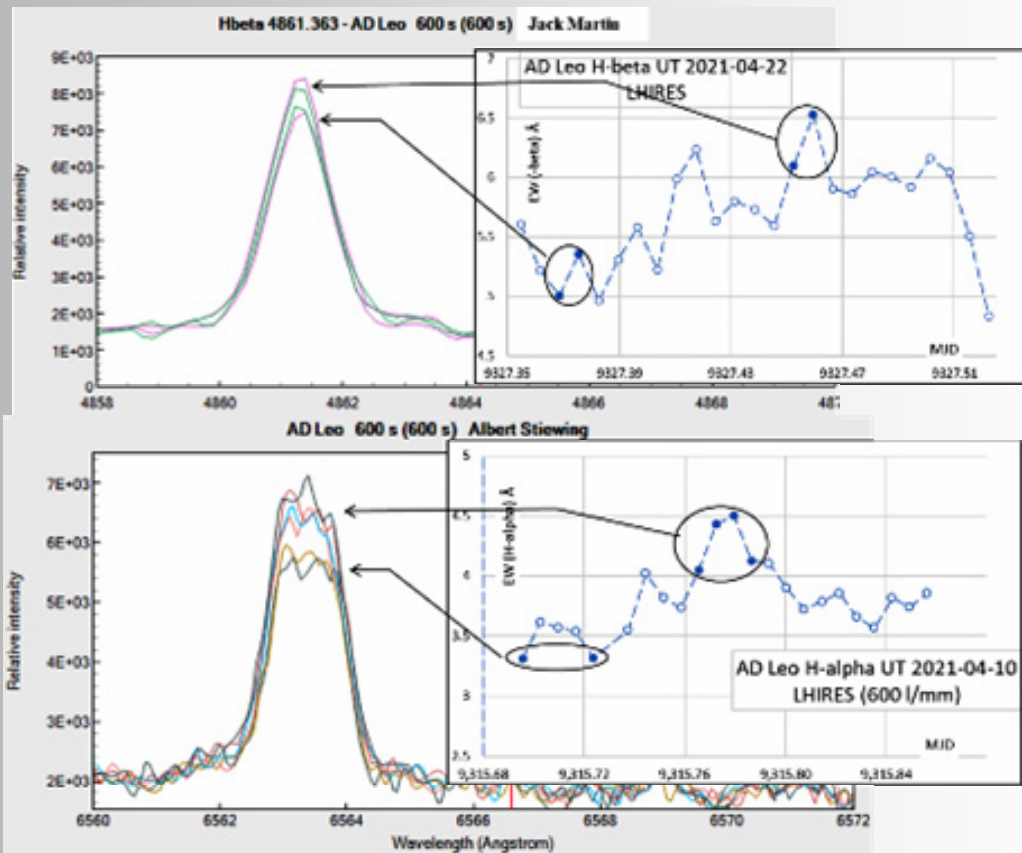
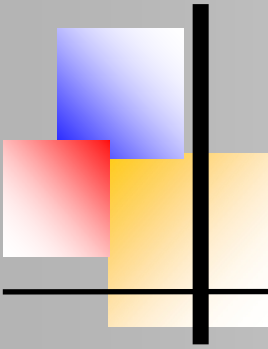


**Fig. 6:** Example high-resolution spectra of H $\alpha$  (top panel) and H $\beta$  (bottom panel), showing the detection of small flare events.



# BAV MAGAZINE SPECTROSCOPY



## Spectroscopy of Stellar Flares

We gathered a limited number of high-resolution spectra. The results, illustrated in Fig. 6, were encouraging: We saw a few small flares in  $H\alpha$  and  $H\beta$  (but not the same flare in both, because our high-resolution spectrographs do not have a wide-enough spectral range to capture  $H\alpha$  and  $H\beta$  simultaneously). Although the SNR of the spectra are quite a bit lower than what is normally wanted (e.g. we get  $\text{SNR} \approx 15$  to  $20$ , versus most projects expect  $\text{SNR} \approx 100$ ), they give us hope of being able to observe and measure line-profile changes during strong flares (assuming that they exist).

### Next Steps

We plan to continue spectroscopic monitoring of flare stars, by selected two or three attractive candidates (one per season) and bringing some additional observers into the project. That should increase the number of flares that we see and enable us to create flare-frequency diagrams and other analyses of the spectral-evolution of the flares. Some observers using UVEX spectrographs have joined us, which presents the exciting prospect of better data on the Ca II (H) and (K) lines, in addition to the Balmer lines of Hydrogen. We wished that we had consistent photometry to augment the spectroscopy during the AD Leo project. We are getting set up for that now and are seeing results such as Fig. 7. This is exciting because the photometry will enable us to flux-calibrate the spectra, translate EW into flare luminosity (emitted power vs. time) and total emitted energy, and correlate “white light” flares with “spectroscopic” flares.

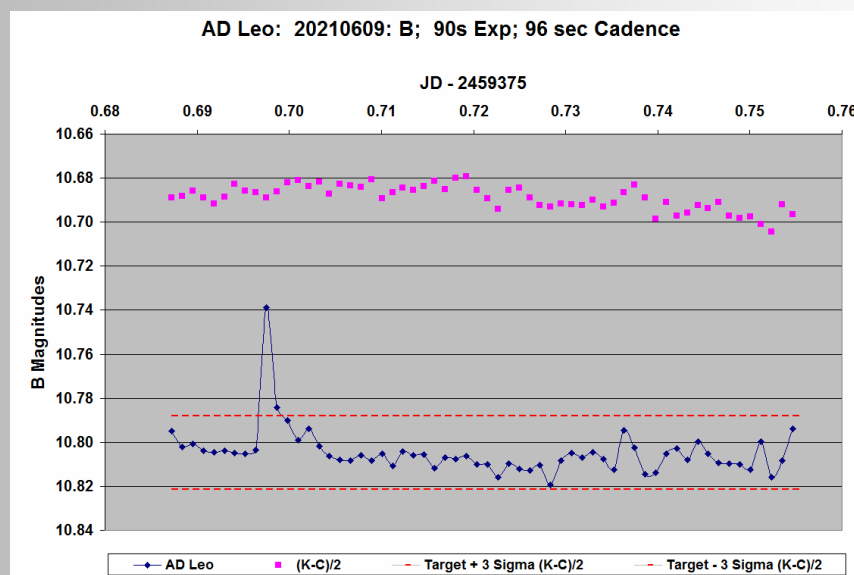
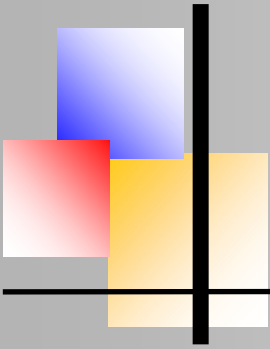


**Fig. 7:** B-band photometry of a flare on AD Leo (by Gary Walker). The 90-second imaging cadence recorded this flare, whose total duration is much shorter than the flares we have been seeing in our time-series spectra (which use a 300-second cadence).



# BAV MAGAZINE SPECTROSCOPY



## Spectroscopy of Stellar Flares

One of our advisors had suggested selecting an earlier spectral-type star as a target, since the lower rate of observable flares makes such stars a tough challenge for professional observatories. We selected BY Dra as a target (SpTy=K4Ve+K7.5Ve), but were “skunked” by terrible weather at all our observing locations.

We have been observing EV Lac (a well-known flare star) extensively for the past few months, and have captured simultaneous photometry (primarily B-band, but some U-band also) and spectroscopy of flares.

We will definitely be back on AD Leo in early 2022. TESS will have AD Leo in its field during Sector 48 (2022-Jan-28 to 2022-Feb-26, in cycle 4), which should provide us with outstanding space-based photometry to correlate with our ground-based measurements.

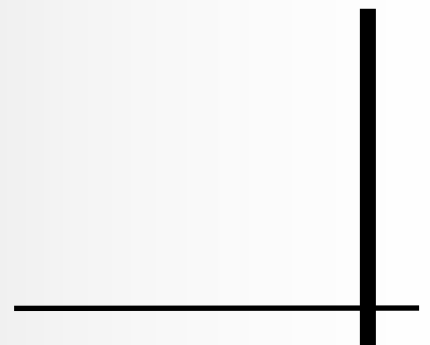
### Conclusions

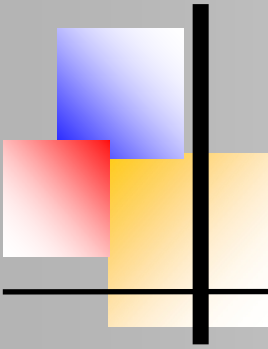
We monitored the M-dwarf star AD Leo to investigate the feasibility of (1) seeing the spectroscopic signature of stellar activity, and (2) characterizing the observed flare-events. Our time-series spectra of AD Leo detected events with stellar-flare signatures, at an average rate of 1 event per 6.1 hours of observing time. We observed the time-evolution of EW (Equivalent Width) during these events and searched for line-profile changes (unsuccessfully, so far).

We conclude that small telescope spectroscopy – at both high- and low-resolution – can detect and characterize stellar flares. Whether these observations can contribute to research on stellar flares is still an open question, but our advisors have been very enthusiastic about our effort and results so far.

Possible avenues include increasing the number of flares observed, confirming the flare-rate on different stars, characterizing flare evolution on short time scales (minutes), and searching for stellar activity cycles.

A video presentation of our project (for the Society for Astronomical Sciences) is available at <https://youtu.be/UuRhAlsfeegg>. Our report is published in the proceedings of the 2021 Symposium of the Society for Astronomical Sciences, which will be on the SAS website soon ([www.SocAstroSci.org](http://www.SocAstroSci.org)).





## The Seyfert Galaxy NGC 2410

Michael Koenig, [www.astro-images.de](http://www.astro-images.de),



### Abstract

In the constellation Gemini, just a few degrees above Castor, stands the galaxy NGC 2410. With the Aladin Viewer of the University of Strasbourg, it is easy to see that it is a barred spiral galaxy, which we observe from obliquely above, with respect to its main plane. The star catalog that Aladin uses by default is the STScI/NASA DigitalSkySurvey. For amateur observers, this fits very well for planning and conducting imaging sessions.

The faintest stars range up to 19 mag. My instrument is an 14" f/6 cassegrain reflector. The LISA spectrograph is equipped with a off-axis guider. In the guider, stars as faint as 16 mag can be seen with a 2 second exposure. The image below shows the guider section, which is only 10' in size. The image was taken at the beginning of the observation, here the telescope was not yet cooled down, so the stars appear quite bloated due to the tube entry.

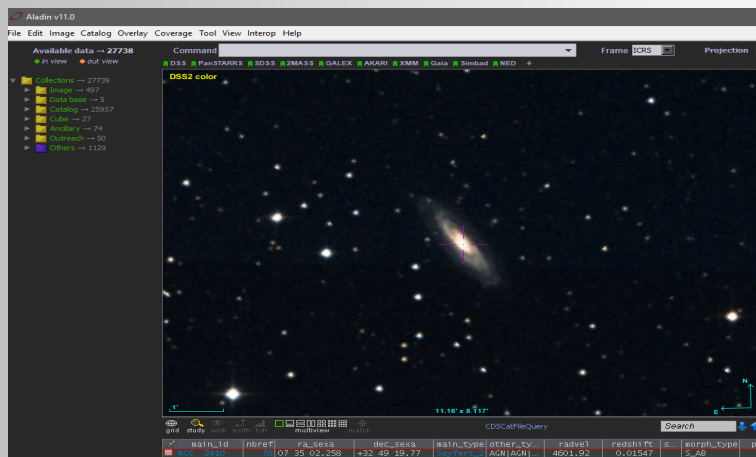
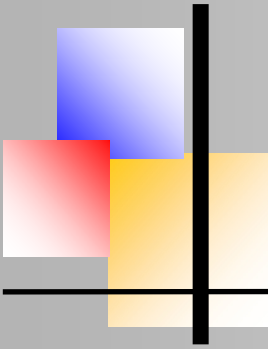


**Fig. 1:** The galaxy NGC 2410; Aladin Viewer of the University of Strasbourg

The surface brightness for NGC2410 is between 13 mag to 14 mag in the optical. For the core I estimate the brightness to 15 mag to 16 mag. SIMBAD gives NGC 2410 17.0 mag in the B-band, 16.3 mag in the V-band and 10.6 mag in the J-band (1,250 nm). The weather allowed only a short session in the evening of 6.1.2022. It was quite clear at 21:00, but clouds were predicted to gather at midnight. I placed the slit in RA direction over the bright nucleus of NGC 2410 and the tracking was done at the bright star standing to the left of the galaxy. 4 spectra were made with a single exposure time of 20 min. The spectra were summed and then further processed in BASSProject.



# BAV MAGAZINE SPECTROSCOPY



The Seyfert Galaxy NGC 2410

The first profile shows the still raw spectrum, so here the instrument response is not yet considered. But you can already see the emission lines sitting on the continuum. And you can also see that these lines are clearly red-shifted.



**Fig. 2:** The slit of the spectrograph was placed in RA direction over the bright nucleus of NGC 2410

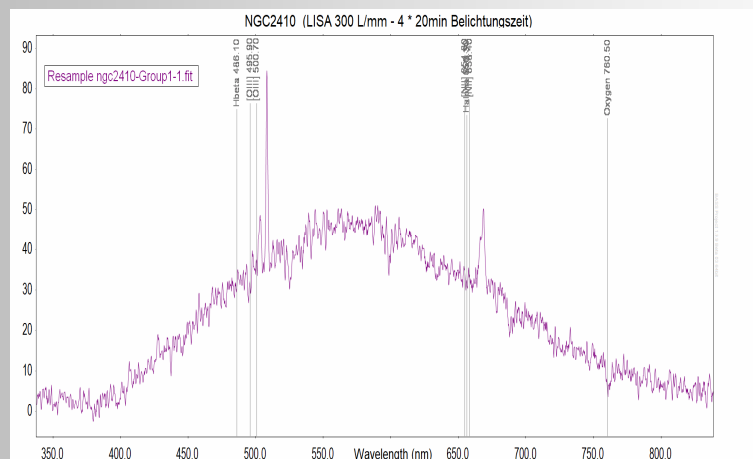
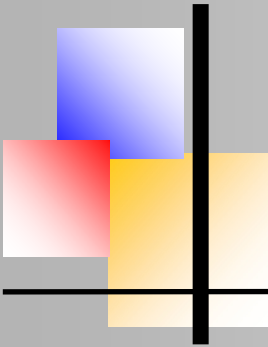


**Fig. 3:** The first profile of the NGC2410 raw spectrum

Especially prominent are the two [OIII] lines, The hydrogen lines are comparatively fainter. The H-beta line can be recognized and the H-alpha line in the red forms together with the two [NII] lines a broad foot of an emission structure. The absorption line at 760.5 nm is due to oxygen in the Earth's atmosphere. This line is not redshifted.



## The Seyfert Galaxy NGC 2410

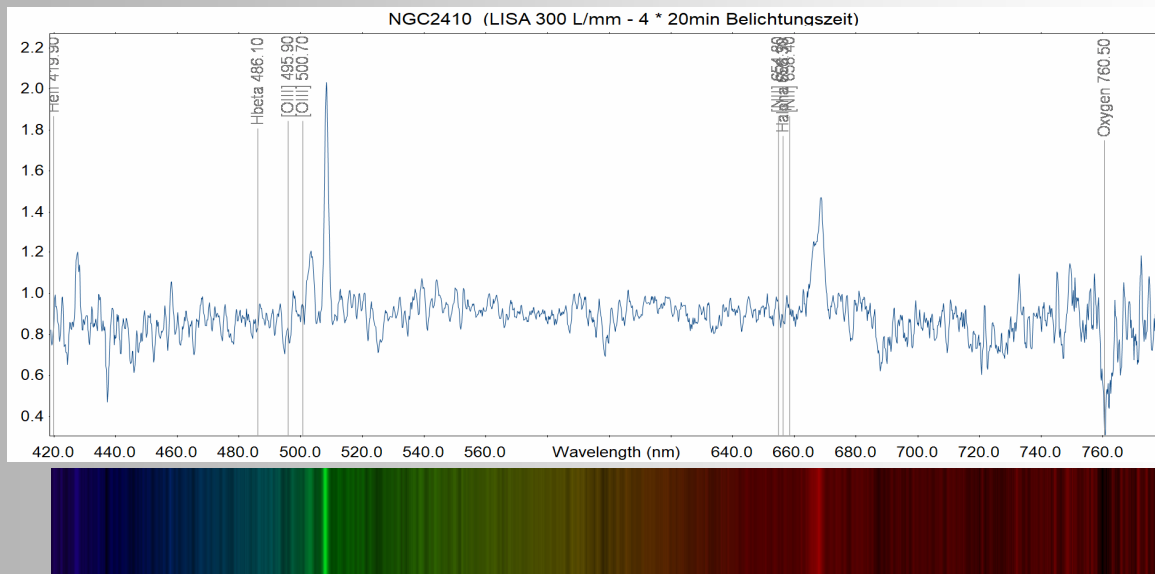


**Fig. 4:** (top): Normalized spectrum (continuum removed) of NG2410;  
(bottom): Synthetic colored spectral band of the spectrum scan. The emission lines are easily seen as bright bands in the colored spectral band. On the far left in the violet a faint line can be seen, which could be a HeII emission.

Due to the fact that the identification of the prominent lines is quite reliable and they are well defined, their exact position can be determined with the help of a Gauss fit. Before this, however, the continuum is removed and the flow is normalized. Thus, a flat course is achieved and thus more reliable values for the determined line positions.

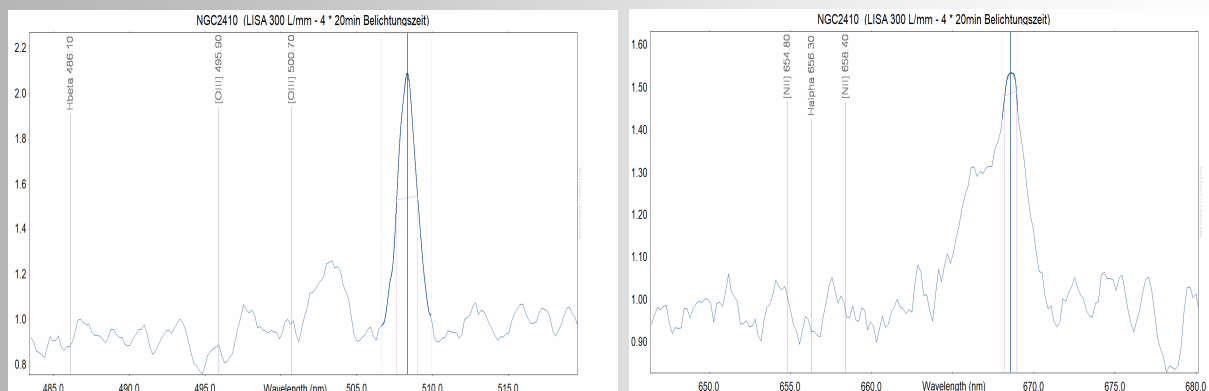
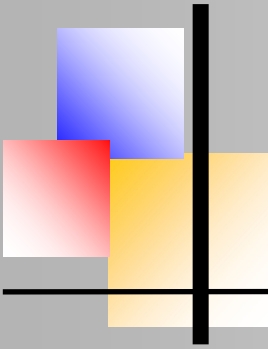


**Fig. 5:** This both continuum corrected spectra shows the sections around the [OIII] (left) and the [NII] lines (right). In the line profiles used in each case one can see the fitted Gaussian function.



# BAV MAGAZINE SPECTROSCOPY



The Seyfert Galaxy NGC 2410

The following measured values are obtained:

Measured Wavelength of the Peaks	Wavelength of rest	Wavelength shift $v/c$
[OIII] 508.322 nm	500.70	0.01528
[NII] 669.569 nm	658.40	0.01554

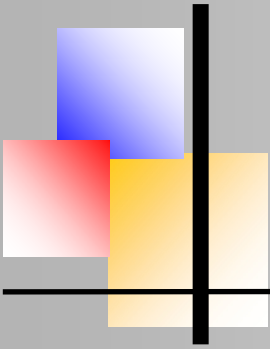
Calculating the average of the two redshifts, we get the escape velocity of 4.608 km/s for NGC 2410 from the measurement of  $v/c$ . Included is the barycentric correction of +2.01 km/s. I estimate the error to be +/- 40 km/s.

If you compare the measured value with the literature value of 4.601.92 km/s, you get a surprisingly exact value, because the deviation is only 0.04%. But this is a coincidence, the error is in the range of 1 to 2%.

The distance of NGC 2410 results to 208 million light years. The size of the barred spiral disk is 150,000 lightyears, which is about the same as the Milky Way. NGC 2410 is part of a small galaxy group (LGG146). It may be that by interactions with the colleagues it could have come to inflow of matter on the supermassive black hole in the center. This machine in the inside is active and produces in the optical the emission lines which can be observed in the spectrum.

This is also the reason why NGC 2410 is counted to the Seyfert galaxies. It was discovered by Carl Seyfert in the 1940s. Within the Seyfert galaxies NGC 2410 is a type-II with slender emission lines. In this type we do not look directly into the center, because it is surrounded by a surrounding dense dust torus. We see only the light reflected in our direction by dense wools located above and below the torus.

These move comparatively slowly, making the lines appear slender. It is different with Seyfert-I types. Here you look into the center and there you see fast circulating clouds. Their velocities reach up to 10,000 km/s and cause a strong line broadening. These enormous widths then show up in the hydrogen lines. At NGC2410 you don't see these lines, fitting nicely to their typification.



## RS Oph – Variation of narrow Na D lines during 2021 outburst

Matthias Kolb, Wuppertal (Germany)



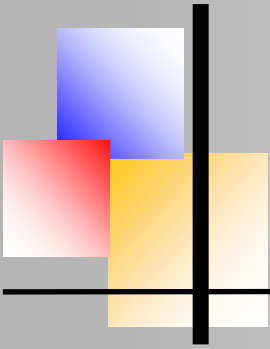
### Abstract

The 2021 outburst of the symbiotic recurring nova (RN) RS Oph has gained a lot of attention both by professional as well as (even more) amateur astronomers. Plenty of spectra with a wide range of resolution were taken and published since August 2021. An overview can be seen in the presentation of Teyssier (2021) and the papers of Munari & Valisa and Zamanov et. al. The spectra during outburst show a lot of interesting aspects, for example the lines from highly ionized atoms like He II or O VI and the specific profile of the H $\alpha$  emission composed by broad and narrow

features. For a detailed explanation for these lines see Teyssier (2021).

The scope of this work is to focus on a specific narrow band absorption line and its development during the outburst: The Na I D line. The reason to focus on this particular line originates from the potential connection between RN like RS Oph and supernovae of Type Ia. F. Patat and co-workers (2011) analysed the narrow band variations of the Na I D, Ca II H&K as well as K I (7699 Å) lines during the previous outburst in 2006. As I cannot print figures from their work here I recommend to reader to look into their paper, in particular figures 2 and 5. Their conclusions are:

- The lines show at least 5 significant features called #1 to #5. Their specific location is given in km/s shift versus the systemic velocity of -40.2 km/sec toward the sun. Two features (#4 at 42 km/s and #5 at 30 km/s) are red-shifted the three first are blue-shifted by approx. 4, 21 and 35 km/s.
- The features #4 and # originate mainly from the local spiral arm of our galaxy, have therefore no connection to RS Oph. Their location and intensities remain constant over time.
- The other three features originate (mainly) from circumstellar matter around the RS Oph system, outside of the stellar orbit of approx. 1.4 au. #1 and #2 come from distances further out and #3 closer to the orbit. This circumstellar matter is considered to be a remnant of previous outbursts of RS Oph.
- These three features, in particular #3 show a significant decline during the first days of the outburst versus the quiescence phase before and also to the following quiescence phase (742 days after outburst). This decline is explained due to the interaction of radiation and / or ejecta of the outburst with the circumstellar medium after the outburst, leading to a local increase in density, change of ionization state and reduction of the emission.
- Although emission of feature #3 goes up again after the outburst, the circumstellar medium is different in the quiescence phase after the 2006 outburst compared to before: The outburst leaves some fingerprints in the circumstellar environment.



## RS Oph – Variation of narrow Na D lines during 2021 outburst

Booth et.al. (2015) have run model calculations for the circumstellar medium of RD Oph as well as model calculations for SN Ia. Impressive pictures from Hubble Space Telescope from 2006 show a bipolar structure of the ejection nearly perpendicular to the orbit plane of the white dwarf and red giant (Harman et al., 2008)

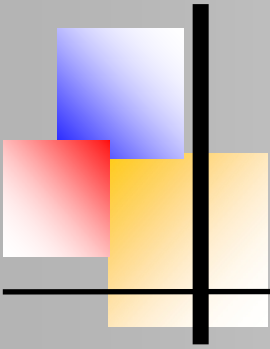
By coincidence, although in 2006, a supernova of type Ia was detected in the spiral galaxy M100 in the constellation of Coma Berenices. Interestingly this SN (as well as few others) do also indicate features at similar blue-shifted distances from the systemic velocities (Patat, 2011). This could be an indication that these supernovae are indeed examples for the single-degeneracy scenario where the precursor of the supernova is a nova like binary system. General believe today is that the majority of SN Ia originate from double-degeneracy scenario with two with dwarfs colliding. In those cases no circumstellar medium should be detected and that seems to be indeed the case for most of the supernovae Ia investigated so far. The new outburst of RS Oph offers the opportunity to look again at the Na D lines and their development since August 2021. I used the ARAS database to select several spectra at reasonably high resolution. None of those spectra came close to the  $R=48,000$  value in Patat et.al, but are around 10,000.

### Evaluation of the Na I $D_1$ line

Out of the many spectra in the database, I took 18 of high resolution, starting June 7, 2019 (794 days before outburst maximum). Last spectrum is from October 29, 2021 (+74 days), certainly not yet at quiescence. Unfortunately the last quiescence spectrum dates back to September 2020, nearly a year before the August 2021 outburst.

The Helium I line at  $5876 \text{ \AA}$  is close to the  $D_2$  line around  $5890 \text{ \AA}$  and this line is increasing significantly during outburst. As the resolution of the spectra is not high enough to completely separate the lines at later times the  $D_1$  line is evaluated as also done in the work from Patat. The spectra show only two features, not the full diversity shown in Patel's paper with 5 significant features. During the later phase there is indeed some separation visible in the blue shifted part. I calculated the difference in km/s for the two major peaks of  $D_1$  and it is typically around 50 km/s (+/- 10) which is in reasonable agreement to the separation of #4/#5 versus #1-#3 in the 2006 case.

Fig. 1 shows the area around the Na D doublet on August 9, 2021 close to the maximum of the outburst. Still visible is the P-Cygni profile of the He I emission line as well as the two major features of the Na D lines with not identical but comparable fluxes. The P-Cygni profile will disappear soon and a broad emission He I line dominates this region of the spectra.



# BAV MAGAZINE SPECTROSCOPY



RS Oph – Variation of narrow Na D lines during 2021 outburst

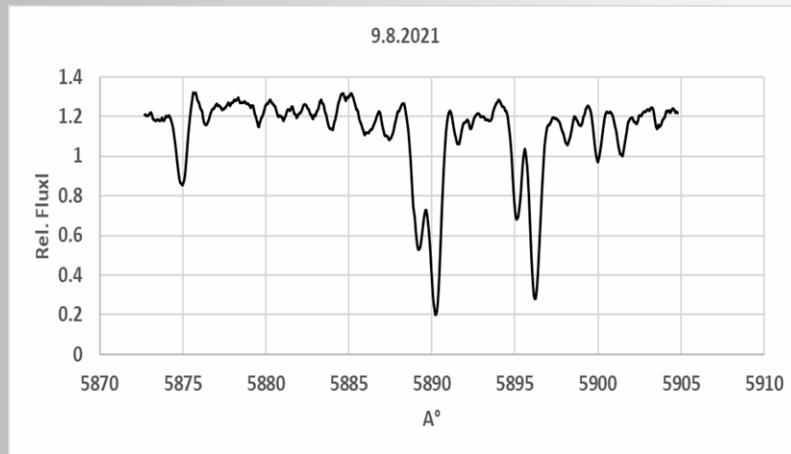


Fig. 1: Part of the spectrum from August 9, 2021 taken by Olivier Thizy.

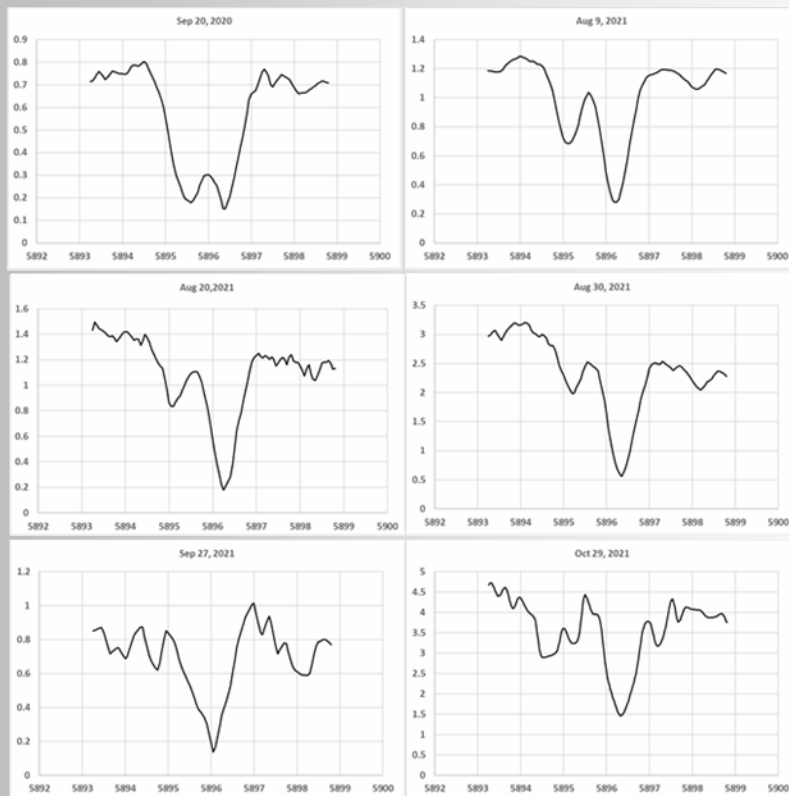
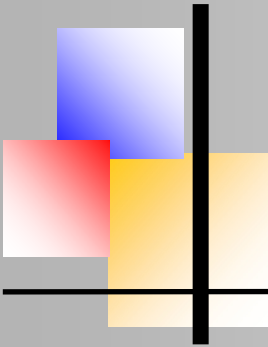


Fig. 2: Spectra from ARAS database taken by Joan Guarro (29.9.20), Stéphane Charbonnel (9.8.21, 30.8.21), Olivier Thizy (20.8.21), Francois Teyssier (30.8.21), Colin Eldridge (29.10.21). Axes as fig. 1.



RS Oph – Variation of narrow Na D lines during 2021 outburst

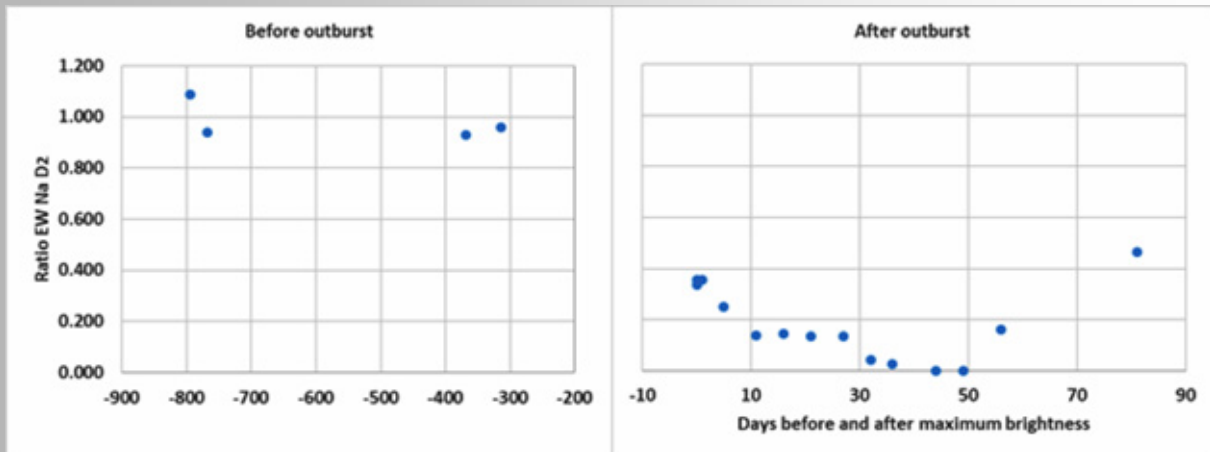


Fig 3: EW of the ratio of the two feature in D<sub>1</sub> during quiescence and after outburst.

## Conclusion

Both Na I D lines show clearly two features before and during outbreak. The intensities of the red-shifted peaks decrease during outbreak strongly and some recovery seems to happen with time. Although, more detailed structures appear in the later spectra. Of course, this analysis cannot confirm neither the origin of the lines nor the interpretation of the mechanism for their development during outbreak. But the phenomenon as such appears similar compared to the 2006 outbreak.

## References

- Booth, R.A., Mohamed, S., Podsiadlowski, P.H., Mon. Not. R. Astron. Soc. 457 (2015) or arXiv:1601.02635v1 (2016)  
Harman, D.J. et al., ASP Conference Series, Vol.401, 2008 or arXiv:0809.4592v2 (2009)  
Patat F., Chugai N. N., Podsiadlowski P., Mason E., Melo C., Pasquini L., A&A, 530, A63 (2011)  
Teysier, F., RS Oph 2021, <http://www.astronomie-amateur.fr/Documents%20Novae/RSOph-2021.pdf> and <https://www.youtube.com/watch?v=7Z4GRxoKFRI>  
Zamanov, R.K. et.al., arXiv:2109.11306v1 (2021)

## Acknowledgements

Spectra from the following observers were taken out of the ARAS database:

Tim Lester, Joan Guarro, Olivier Thizy, Stéphane Charbonnel, Olivier Garde, Olivier Thizy, Colin Eldridge, and Francois Teysier

<https://ui.adsabs.harvard.edu/abs/2019CoSka..49..217T/abstract>.

[http://www.astrosurf.com/aras/Aras\\_DataBase/DataBase.htm](http://www.astrosurf.com/aras/Aras_DataBase/DataBase.htm).



## The V/R-Ratio in zeta Tau

Ernst Pollmann, eMail: ernst-pollmann@t-online.de



### Abstract

The ratio of the violet peak flux (V) to the red peak flux (R), the so-called V/R ratio of the H $\alpha$  emission shows a significant decrease in amplitude from April 1991 to January 2010, accompanied by a decrease in the H $\alpha$  equivalent width (EW). Simultaneously with the significant change of the V/R ratio from V<R to V>R, the H $\alpha$  emission exhibits as a triple-peak profile during a phase of disappeared V/R cycles. This phase of the ended V/R variations from around mid-January 2010 (JD 2455215) made it possible to investigate the behavior of the central absorption (CA) in the H $\alpha$  emission. The CA period of 153d we found, and its small time difference from the orbital period of 133d can be interpreted as confirmation of the “disk nodding” found by Schaefer et al (2010).

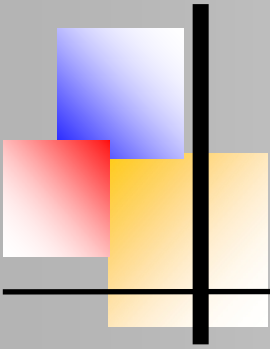
### Introduction

The fact that  $\zeta$  Tau has a binary companion in a 133-day orbit (Ruždjak et al. 2009) and (Bjorkman et al. 2000), likely means that any tilt of the Be star's disk is modulated by the tidal force of the companion. Approximately twice per orbit an inclined disk experiences a tidal torque in the direction of alignment with the orbit, which results in a nodding motion being seen, which has been proven by Schaefer et al. (2010) and by Collins & Scher (2002) in the precessing disks and the jets of massive x-ray binary stars (e.g. SS 433).

### Observation

The results presented here should be understood as a natural continuation of earlier investigations to the V/R variability by Pollmann & Rivinius (2008). They have been obtained by use of classical slit spectrographs (spectral resolution R between 15000 and 20000) and telescopes with apertures of 30 to 50 cm. The spectra have been reduced predominantly with the software VSpec by Desnoux (2019). For this investigation only spectra have been considered with a signal to noise ratio (S/N) better than 100. The spectra were normalized by manually defining suitable continuum points in the spectral range 6500 to 6700Å using optimal spline functions. The wavelength calibration was derived using the telluric absorption lines in the H $\alpha$  range with an accuracy of about  $\pm 0.05\text{Å}$ .

The violet A peak flux (V) and the red B peak flux (R), both related to the normalized continuum, enables to define the so-called V/R ratio of the H $\alpha$  emission (Fig. 1). The depth of the central absorption CA in Fig. 1 is defined as difference CC' of the local normalized continuum (=1) either to the line flux minimum under the continuum (CA < 1), or to the line



flux minimum above the continuum ( $CA > 1$ ). In the normalized and calibrated spectra, the  $H\alpha$  equivalent width is obtained by integrating the spectral range from 6520-6610Å. The spectra have been cleaned from the telluric water line with the software SpectroTools of Schlatter (2022). It uses a method developed by Seifahrt et al. (2010). Spectral Tools creates a model atmosphere by removing a high resolution spectrum of water, creating as close as possible the conditions prevailing when the star spectrum was recorded.

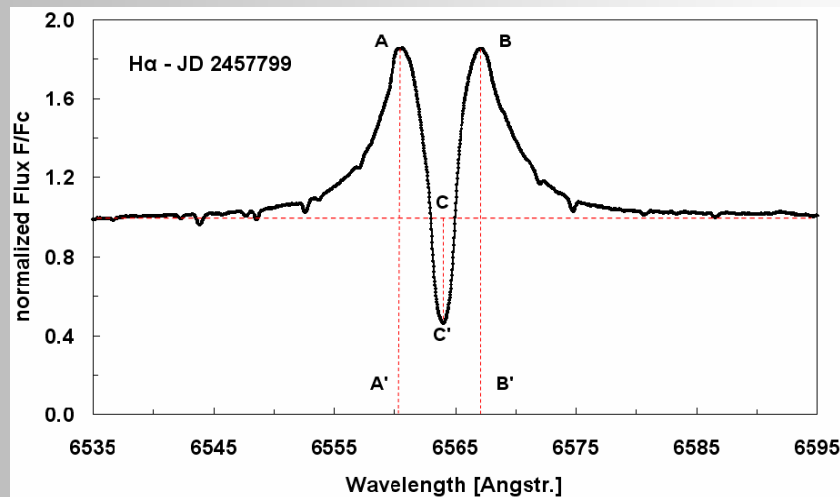


**Fig. 1:** Definition of the measured parameters in the  $H\alpha$  line profile: (AA') and (BB') emission peaks, depth of the central absorption  $CA = (CC')$ . The horizontal line marks the normalized continuum.

## Results

The V/R monitoring of the  $H\alpha$  emission of  $\zeta$  Tau (top panel of Fig.2) from April 1991 (JD2448348) to February 2022 (JD2459614) shows a clear decrease of the V/R amplitude within a period from April 1991 to January 2010 ( $\sim 19$  years). The question is what are the physical causes in the Be star disk that have led to this decrease. In general, the periodically variable V/R ratio at  $\zeta$  Tau represents local density differences (one-arm density wave) in the precessing Be star disk (period  $\sim 1400$  days; see period analysis Fig. 3).

The absence of the V/R variations certainly means that the previous, inhomogeneous density contrast (one-armed density wave) has been reduced by homogenization. It is interesting that this reduction in amplitude is accompanied by a decrease of the  $H\alpha$ -EW (see bottom panel of Fig. 2) and, therefore, the total mass/volume of the circumstellar disk. According to Ruždjak et al. (2009), however, this type of V/R variation can also end without the EW decreasing.

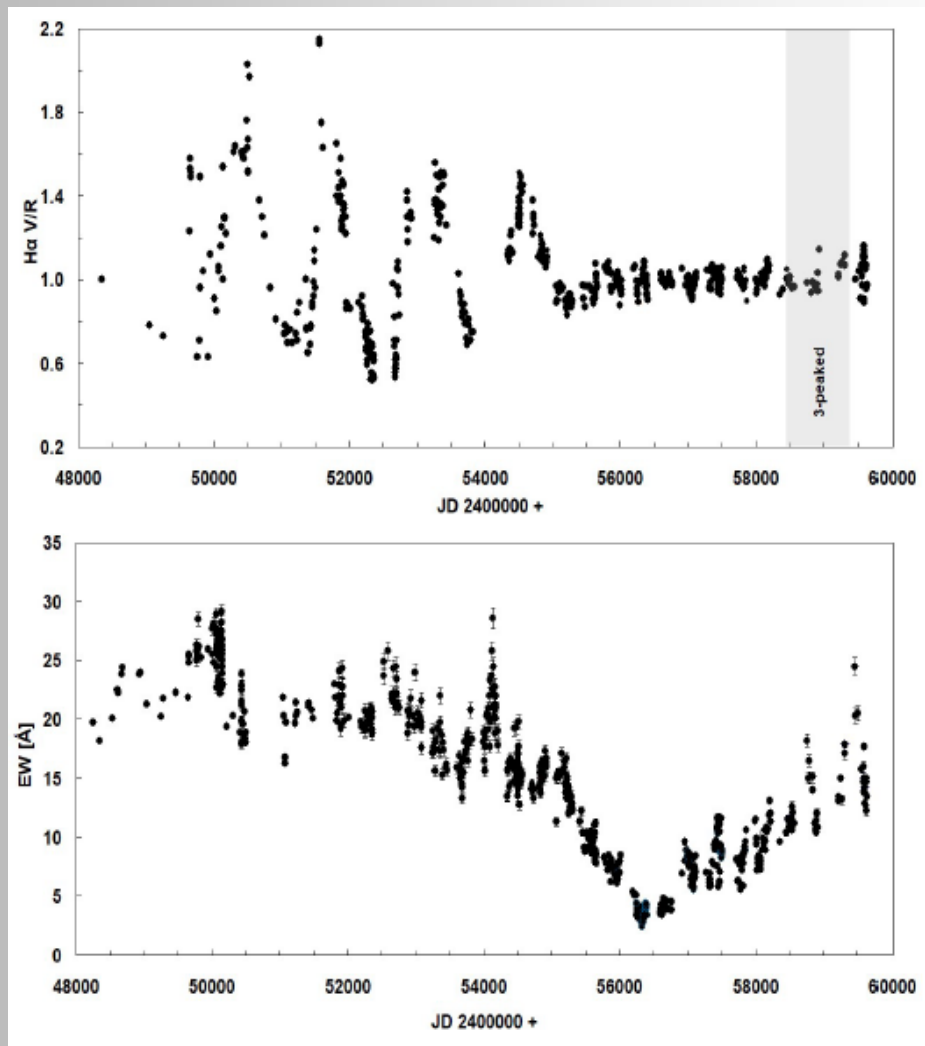
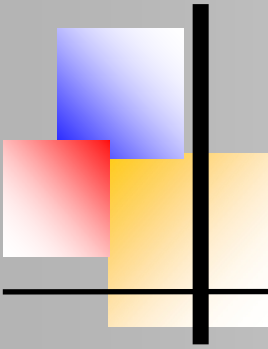


**Fig. 2:** The H $\alpha$  V/R (top) and EW (bottom) monitoring from April 1991 to March 2022. The black dots are contributed spectra from the ARAS observer consortium. The gray bar (top panel) represents the range of triple-peak spectra we found.

A period analysis ( $\log V/R$ ) of the active V/R phase from January 1991 to January 2010 in Fig. 3 resulted in a cycle time of  $1398 \pm 10$  d, i.e. about 3.8 years. (Ephemeris:  $T_0 = \text{HJD}2448664 + 1398 * E$ , where  $T_0$  is the time when  $V/R = 1$ ). While this period is shorter than Okazaki's (1997) 5-7 year period from observations between 1960 and 1993, it is in good agreement with the 4.25 year cycle time of Rivinius et al. (2006) from observations between 1991 and 2003 (Bjorkman, Miroschnichenko & Krugov, 2000).

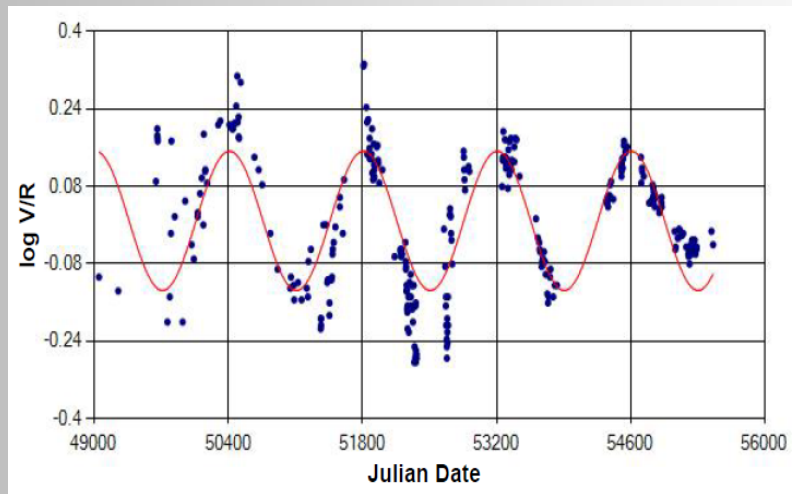
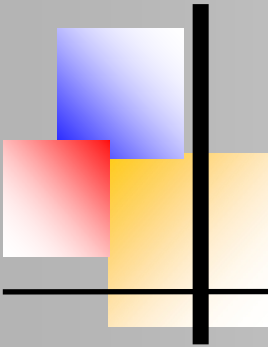


**Fig. 3:** V/R period analysis ( $\log V/R$ ) of the active V/R phase from January 1991 to January 2010. Period = 1398 d;

Occasionally, however, the central absorption (CA) in the  $H\alpha$  emission can weaken or even disappear, so that the emission line profile can become more complicated and can be split into sub-peaks, or even appear as a triple-peak structure as is shown in Fig. 4.

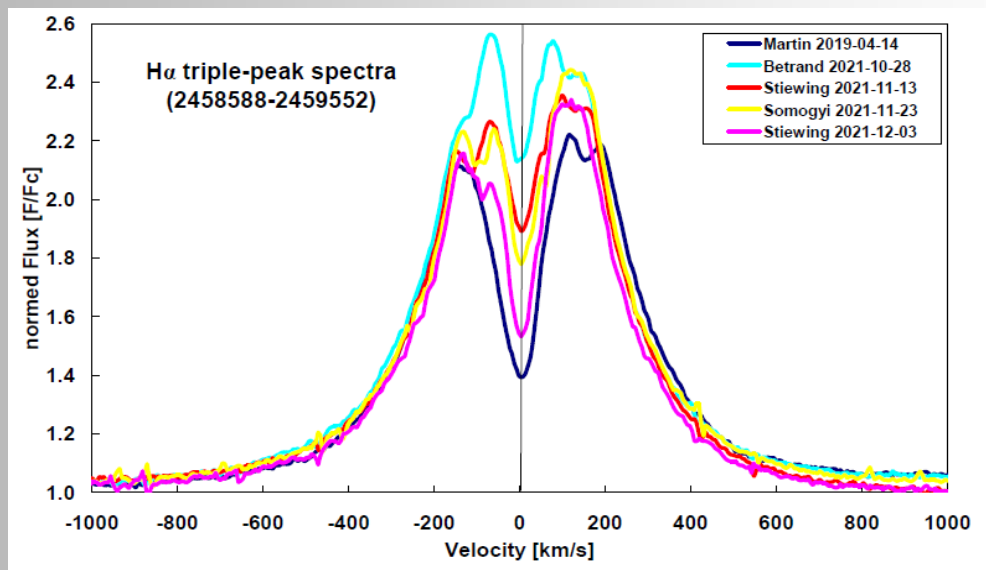
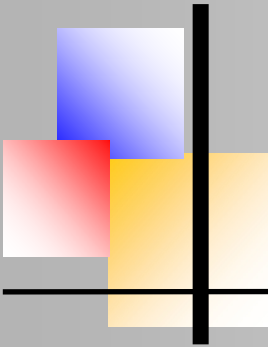


**Fig. 4:** Triple-peaked structures in the  $H\alpha$  emission profile; Period: April (JD 2458588) to December 2021 (JD 2459552)



These triple-peak structures have been found by Escolano et al. (2015) in  $\log(V/R)$  monitoring (Fig. 5) during three V/R cycles (grey bars in bottom panel of Fig. 5). In comparison, we found in our spectral monitoring in Fig. 2 (top panel, gray bars) within the phase of the ceased, previously pronounced V/R cycle activity between JD 2458588 and JD 2459552 additional triple-peak profiles with varying characteristic of intensity as it is shown in Fig. 4.

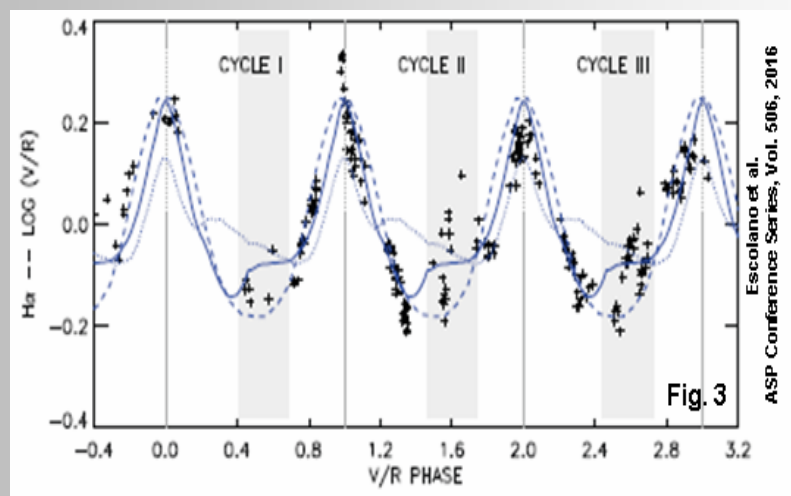
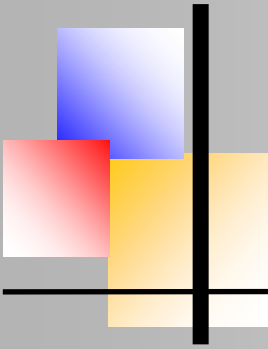


**Fig. 5:** Triple peak structures (marked grey) in the  $\log(V/R)$  monitoring by Escolano et al. (2015) (with friendly permission by C. Escolano)

The reasons for the emergence of these profile structures are still unclear. In general, they appear in the transition phases from  $V < R$  to  $V > R$ , but not vice versa. The phase of absent V/R variations shown in Fig. 1 from mid-January 2010 (JD 2455215) to the present time has prompted us to study the behavior of the central absorption dip (CA) in the  $H\alpha$  emission (definition of this parameter in Fig. 1).

Because the system is being observed roughly equator-on [ $\sim 70^\circ$ , Jarad (1987), Schaefer et al. (2010)], the depth of the  $H\alpha$  CA is an indicator of a varying inclination of the disk. While the  $H\alpha$  emission line samples the circumstellar disk as a whole, the region probed by the central absorption CA is restricted to the line of sight. The diagnosis of the absorption depth reflects the structure and dynamics of the disk in the observer line of sight. The spectral resolution of the spectra used for this investigation was between  $R \sim 15000$ -20000.

Fig. 6 shows the time behavior of the CA between March 2011 and March 2022. A phased-dispersed-minimization (PDM) period analysis was carried out for the section from JD 2456500 to the present time (March 2022). The period analysis as phase diagram in Fig. 7, clearly



illustrates the periodic CA character with a period of 153.5 days (Ephemeris:  $T_0 = \text{HJD } 2456531 + 153.5 * E$ ).

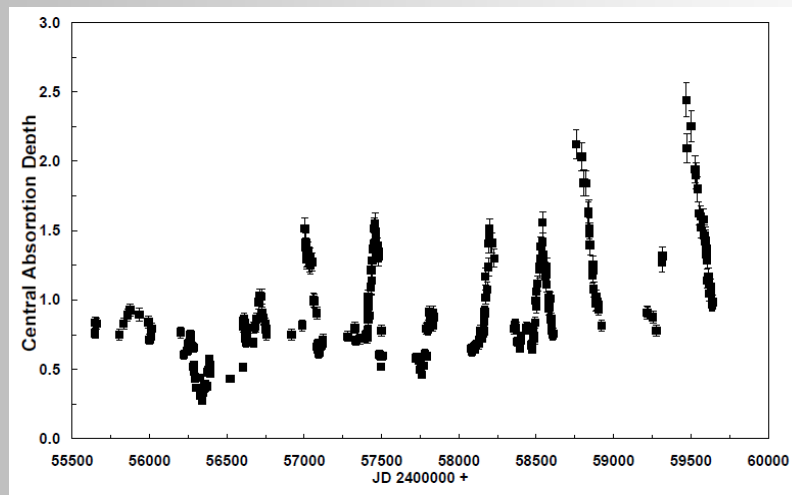


**Fig. 6:** CA monitoring from March 2011 (JD 2455649) to March 2022 (JD 2459648)

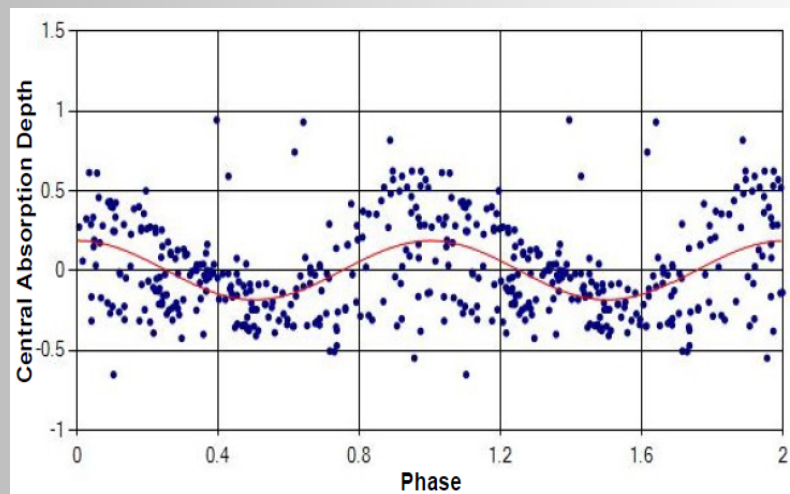
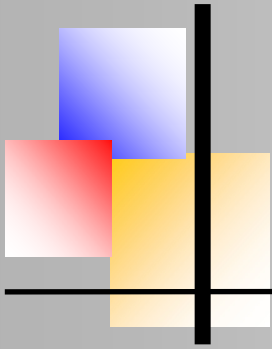


**Fig. 7:** CA-PDM period analysis; time span: August 17/2013 (JD 2456521) to February 05/2022 (JD 2459616).

Up to now, real V/R phase-locking in Be star has always been assumed as a consequence of a density wave. Instead, simulations by Štefl et al. (2007) point out a tide-bound in the case of eccentric binaries, tidal perturbations can develop with a period that is slightly longer than the orbital period.



Although one cannot detect the secondary component of the binary directly, and assumes that the inclination angle of the orbital plane of the binary is the same as that of the circumstellar disk (Tycner et al. 2004), the question remains to what extent the findings can also be transferred to the varying depth of the absorption depression CA. However, the small time difference between our found 153.5d period and the orbital period of 133 days could possibly be justified with the simulation findings of Štefl et al. (2007).

**Observer consortium** (contact address: [ernst-pollmann@t-online.de](mailto:ernst-pollmann@t-online.de))

Observers: O. Garde, K. Graham, O. Thizy, J. Guarro, T. Heidmann, T. Lester, A.  
Favaro, E. Pollmann, Ch. Buil, C. Sawicki, E. Bertrand, E. Bryssinck, B. Koch, B.  
Mauclaire, St. Charbonell, F. Houpert, J. Martin, A. Stiewing, K. Alich, J. N. Terry, A. Maetz,  
P. Somogyi

**Acknowledgement**

I am very grateful to Prof. Dr. Anatoly Miroshnichenko (University of North Carolina at Greensboro), the editors and referee for the critical and helpful support in editing this paper.

**References**

- Bjorkman, K. S., Miroshnichenko; A. S., Krugov, V. D., 2000, <https://ui.adsabs.harvard.edu/abs/2000AAS...196.050B/abstract>
- Collins, G. & Scher, R. W., 2002, MNRAS, 336, 1011
- Desnoux, V., 2019 ; <http://astrosurf.com/vdesnoux/>
- Escolano, C., Carciofi, A. C., Okazaki, A. T., Rivinius, Th., Baade, D., Štefl, S., 2015, A&A 576, A112, DOI: 10.1051/0004-6361/201425446
- Jarad, M. M. 1987, Ap&SS, 139, 83
- Okazaki, A., 1997, A&A 318, 548
- Pollmann, E. & Rivinius, Th., 2008, IBVS No. 5813
- Rivinius, Th., Štefl, S, Baade, D.: 2006, A&A 459, 137
- Ruždjak D. et al., 2009, A&A 506, 1319-1333
- Schlatter, P., 2022; [peterschlatter.ch/SpectroTools2022/SpectroTools.zip](http://peterschlatter.ch/SpectroTools2022/SpectroTools.zip)
- Seifahrt, A. et al., 210, <https://www.eso.org/sci/publications/messenger/archive/no.142-dec10/messenger-no142-21-24.pdf>
- Štefl, S., Okazaki, A. T., Rivinius, T., Baade, D. 2007, Active OB-Stars: Laboratories for Stellar and Circumstellar Physics, ASP Conf. Series 361, 274
- Schaefer, G., H., et al., 2010, The Astronomical Journal, 140:1838–1849
- Tycner, Ch., A. R. Hajian, J. T. Armstrong, J. A. Benson, G. C. Gilbreath, D. J. Hutter, J. B. Lester, D. Mozurkewich, T. A. Pauls, 2004, The Astronomical Journal, 127:1194-1203